

# CHARA Array Measurements of the Angular Diameters of Exoplanet Host Stars

Ellyn K. Baines, Harold A. McAlister, Theo A. ten Brummelaar, Nils H. Turner, Judit Sturmann, Laszlo Sturmann, & P. J. Goldfinger

*Center for High Angular Resolution Astronomy, Georgia State University, P.O. Box 3969, Atlanta, GA 30302-3969*

baines, hal@chara.gsu.edu; theo, nils, judit, sturmann, pj@chara-array.org

Stephen T. Ridgway

*Kitt Peak National Observatory, National Optical Astronomy Observatory, P.O. Box 26732, Tucson, AZ 85726-6732*

ridgway@noao.edu

## ABSTRACT

We have measured the angular diameters for a sample of 24 exoplanet host stars using Georgia State University's CHARA Array interferometer. We use these improved angular diameters together with *Hipparcos* parallax measurements to derive linear radii and to estimate the stars' evolutionary states.

*Subject headings:* infrared: stars — planetary systems — stars: fundamental parameters — techniques: interferometric

## 1. Introduction

Nearly 300 exoplanet systems are now known, discovered via radial velocity surveys and photometric transit events. Most known exoplanet host stars are Sun-like in nature, and their planets have minimum masses comparable to Saturn with orbital semimajor axes ranging from 0.04 to 6.0 AU (Marcy et al. 2005), painting pictures of planetary systems very different from our own.

---

For preprints, please email baines@chara.gsu.edu.

Many exoplanet host stars’ angular diameters have been estimated using photometric or spectroscopic methods. For example, Ribas et al. (2003) matched 2MASS infrared photometry to synthetic photometry in order to estimate stellar temperatures, which then produced angular diameter estimations. Fischer & Valenti (2005) performed the first uniform spectroscopic analysis for all the exoplanets’ host stars known at the time as well as for a large sample of single stars. They determined the effective temperature  $T_{\text{eff}}$ ,  $\log g$ ,  $v \sin i$ , and metallicity for 1040 FGK-type stars to check if there were any correlations between stellar metallicity and the presence of planets and found a rapid rise in the fraction of stars with planets for high-metallicity stars. They calculated stellar radii using stellar luminosities derived from  $T_{\text{eff}}$ , *Hipparcos* parallaxes, and a bolometric correction.

These methods are useful for estimating stellar sizes, but are inherently indirect in nature. Interferometric observations directly measure the angular diameters for these stars, which, in conjunction with parallaxes, lead to linear radii.

## 2. Interferometric Observations

The target list was derived from the general exoplanet list using declination limits (north of  $-10^{\circ}$ ) and magnitude constraints. The stars needed to be brighter than  $V = +10$  in order for the tip/tilt subsystem to lock onto the star and brighter than  $K = +6.5$  so fringes were easily visible. This reduced the exoplanet list to approximately 80 targets, and we obtained data on 24 of them over multiple observing runs spanning 2004 January to 2007 September (see Table 1).

The stars were observed using the Center for High Angular Resolution Astronomy (CHARA) Array, a six-element Y-shaped interferometric array located on Mount Wilson, California (ten Brummelaar et al. 2005). The Array presently employs visible wavelengths (470-800 nm) for tracking and tip/tilt corrections and near infrared bands ( $H$  at  $1.67 \mu\text{m}$  and  $K'$  at  $2.15 \mu\text{m}$ ) for fringe detection and data collection. All observations were obtained using the pupil-plane “CHARA Classic” beam combiner in the  $K'$ -band, except observations of HD 189733, which were obtained using the  $H$ -band. The observing procedure and data reduction process employed here are described in McAlister et al. (2005).

Most observations were taken using the longest baseline the CHARA Array offers, 331 m for the S1-E1 pair of telescopes, due to its sensitivity in measuring stellar diameters<sup>1</sup>. If no

---

<sup>1</sup>The three arms of the Array are denoted by their cardinal directions: “S” is south, “E” is east, and “W” is west. Each arm bears two telescopes, numbered “1” for the telescope farthest from the beam combining

S1-E1 data were obtained, the observations with the longest available baseline were used in the angular diameter measurement. Table 1 lists the exoplanet host stars observed, their calibrators, the baseline used, the dates of the observations, and the number of observations obtained. More information on the transiting planet system HD 189733 can be found in Baines et al. (2007).

We used the standard calibrator-target-calibrator observing pattern so that every target was flanked by calibrator observations made as close in time as possible. This allowed us to calculate the target’s calibrated visibilities from the raw visibilities of the target and calibrator. Acceptable calibrators were chosen to have expected visibility amplitudes greater than 85% on the baselines used, and the high visibilities meant the calibrators were nearly unresolved. Therefore, uncertainties in the calibrator’s diameter do not affect the target’s diameter calculation as much as if the calibrator star had a significant angular size on the sky.

Another small source of potential systematic error in the target’s diameter measurement arises from limb-darkening effects, though the error is on the order of a few percent and is not as significant an effect in the  $K'$ -band as it would be for measurements in visible wavelengths (Berger et al. 2006). For barely resolved calibrators, this effect is negligible.

In an effort to find reliable calibrators, we made spectral energy distribution (SED) fits based on published  $UBVRIJHK$  photometric values for each calibrator to establish diameter estimates and to check if there was any excess emission associated with a low-mass stellar companion or circumstellar disk. Calibrator candidates with variable radial velocities reported in the literature or with any other indication of a possible companion were discarded even if their SEDs displayed no characteristics of duplicity.

Limb-darkened angular diameter estimates for the calibrators were determined using Kurucz model atmospheres<sup>2</sup> based on  $T_{\text{eff}}$  and  $\log g$  values obtained from the literature. The models were then fit to observed photometric values also from the literature after converting magnitudes to fluxes using Colina et al. (1996) for  $UBVRI$  values and Cohen et al. (2003) for  $JHK$  values. See Table 2 for the  $T_{\text{eff}}$  and  $\log g$  used and the resulting limb-darkened angular diameters.

Table 3 lists the Modified Julian Date (MJD), baseline ( $B$ ), position angle ( $\Theta$ ), calibrated visibility ( $V_c$ ), and error in  $V_c$  ( $\sigma_{V_c}$ ) for each exoplanet host star observed. It shows the information for one star here as an example, and the full table is available on the electronic

---

laboratory and “2” for the telescope closer to the lab.

<sup>2</sup>Available to download at <http://kurucz.cfa.harvard.edu>.

version of the *Astrophysical Journal*.

### 3. Angular Diameter Determinations

The observed quantity of an interferometer is defined as the squared visibility, though we use the unsquared visibility ( $V$ ) in our calculations here. Diameter fits to visibilities were based upon the uniform disk (UD) approximation given by

$$V = \frac{2J_1(x)}{x}, \quad (1)$$

where  $J_1$  is the first-order Bessel function and

$$x = \pi B \theta_{\text{UD}} \lambda^{-1}, \quad (2)$$

where  $B$  is the projected baseline at the star's position,  $\theta_{\text{UD}}$  is the apparent UD angular diameter of the star, and  $\lambda$  is the effective wavelength of the observation<sup>3</sup> (Shao & Colavita 1992). The limb-darkened (LD) relationship incorporating the linear limb darkening coefficient  $\mu_\lambda$  (Hanbury-Brown et al. 1974) is given by:

$$V = \left( \frac{1 - \mu_\lambda}{2} + \frac{\mu_\lambda}{3} \right)^{-1} \times \left[ (1 - \mu_\lambda) \frac{J_1(x)}{x} + \mu_\lambda \left( \frac{\pi}{2} \right)^{1/2} \frac{J_{3/2}(x)}{x^{3/2}} \right]. \quad (3)$$

The limb-darkening coefficient was obtained from Claret et al. (1995) after adopting the  $T_{\text{eff}}$  and  $\log g$  values required for each star observed. The resulting angular diameters and other relevant parameters are listed in Table 6. The average difference between the UD and LD diameters are on the order of a few percent, and the final angular diameters are little affected by the choice of  $\mu_\lambda$ . A 20% change in  $\mu_\lambda$  produced at most a 0.6% difference in the angular diameter calculation, so even if the  $T_{\text{eff}}$  and  $\log g$  are not well constrained and therefore  $\mu_\lambda$  is not precisely known, the effect on the LD diameter ( $\theta_{\text{LD}}$ ) will not be significant. Figure 1 shows an example of a diameter fit to calibrated visibilities. Figures 2-24 are available in the electronic edition of the *Astrophysical Journal*.

It was assumed that the visibility curve went to unity at a baseline of 0 m and this carried certain implications. For instance, it was assumed the exoplanet host star was a single star and did not host an unseen stellar companion. A companion check was performed for the stars by studying any possible systematics in the single-star uniform-disk fit errors and

---

<sup>3</sup>Because the flux distributions for these stars in the  $K'$ -band are in the Rayleigh-Jeans tail, there are no significant differences in the effective wavelengths for stars of differing spectral types.

by searching for separated fringe packets (Farrington & McAlister 2006), and the stars all appeared to be single. Another assumption was that the calibrator star’s angular diameter was known and could be used to calibrate the target star’s visibilities. If the calibrated visibilities exceeded 1 for a given dataset, that calibrator was discarded and the target star was observed again with a new calibrator.

For each  $\theta_{\text{LD}}$  fit, the errors were derived via the reduced  $\chi^2$  minimization method: the diameter fit with the lowest  $\chi^2$  was found and the corresponding diameter was the final  $\theta_{\text{LD}}$  for the star. The errors were calculated by finding the diameter at  $\chi^2 + 1$  on either side of the minimum  $\chi^2$  and determining the difference between the  $\chi^2$  diameter and  $\chi^2 + 1$  diameter.

Table 6 lists the parameters  $T_{\text{eff}}$  and  $\log g$  from spectroscopic studies that define the limb-darkening coefficient  $\mu_\lambda$ .  $\theta_{\text{UD}}$  was converted to  $\theta_{\text{LD}}$  using  $\mu_\lambda$ , and the combination of  $\theta_{\text{LD}}$  and the *Hipparcos* parallax (van Leeuwen 2007) led to a linear radius for the star. Table 6 also includes LD diameters estimated from SED fits ( $\theta_{\text{SED}}$ ) as a comparison to the measured diameters. The sources for the photometry used are listed in Table 5 and is available online.  $R_{\text{standard}}$  represents the radius expected from the spectral type listed in the second column.

### 3.1. Estimated versus Measured Stellar Diameters

To check the correspondence between the estimated and measured diameters, Figure 25 plots  $\theta_{\text{LD}}$  versus  $\theta_{\text{SED}}$ . At diameters  $\gtrsim 0.6$  mas, the errors for  $\theta_{\text{LD}}$  become smaller than those for  $\theta_{\text{SED}}$ . This is to be expected, as the smaller diameters are nearing the resolution limit of the CHARA Array, and the uncertainties will be larger for these measurements.

In order to characterize the scatter in the diameters, the standard deviation  $\sigma$  of the quantity  $(\theta_{\text{LD}} - \theta_{\text{SED}})$  was determined and was then divided by  $\theta_{\text{SED}}$  for each star. Then all the  $\sigma/\theta_{\text{SED}}$  were averaged together, with a resulting value of 12%. This indicates a fairly good correspondence between the estimated and measured diameters.

## 4. Combining Stellar Radii from Interferometry and Eclipsing Binary Systems

It was of particular interest to combine interferometrically-measured stellar radii and radii determined using other direct means in order to check their compatibility. Some of the most precise stellar radii result from measuring detached, double-lined eclipsing binary systems, as described in Andersen (1991). His sample encompasses all spectral types from O8 V to M1 V and includes one system of two evolved stars. The errors in the radius measurements are  $\leq 2\%$ , and the values are presumed to be valid for single stars.

Figure 26 shows the stellar radii measured from eclipsing binaries and the exoplanet host stars’ linear radii measured here with errors <15%. The Andersen sample has few G and K-dwarfs and our work helps better populate the low-mass range by tripling the number of stellar radii measurements in the  $0.5 \leq (B-V) \leq 1.0$  portion of the plot. The radii measured from eclipsing binaries support the validity of the interferometric measurements. Though 21 stars measured here have linear radii errors <15%, 19 are shown in Figure 26. The remaining targets are HD 59686, a K2 III star, and HD 104985, a G9 III star. The figure demonstrates that many stars in our and the Andersen sample are post-zero-age-main-sequence (ZAMS) objects.

#### 4.1. Separating Dwarfs and Subgiants

Interferometrically-derived radii may reveal the beginnings of post-main-sequence evolution for stars previously classified as dwarfs. Figure 27 plots the stars listed in Table 6 on a color-magnitude plot except for the giants in the sample (HD 13189, HD 59686, and HD 104985). Over half the stars lie on a fairly well-defined main-sequence (M-S) and their measured radii generally match the expected values (see Figure 27). Because there will be some spread in the M-S due to stars having a non-zero age, we are concentrating on the more evolved cases below.

Five of the stars were previously classified as subgiants and, as expected, lie well off the M-S. HD 10697, HD 38529, HD 177830, and HD 190228 were labeled as subgiants by the papers listed in Table 6, and observations confirm the classification. The fifth star, HD 11964, was given a G5 spectral type with no luminosity class. Its measured radius is over twice that expected for a G5 dwarf, and so is most likely a subgiant.

Another group of stars previously classified as dwarfs show measured radii that substantially exceed what is expected from the stars’ spectral types as given by Cox (2000) and show indications of post M-S evolution. These stars are:

*HD 19994:* Mayor et al. (2004) classified this star as an F8 V star when the planetary system was discovered. Its measured radius is  $\sim$ 60% larger than that expected for a standard F8 dwarf star.

*HD 23596:* No luminosity class was assigned to HD 23596 by the *SIMBAD Astronomical Database*, only a spectral type of F8. Its measured radius is  $\sim$ 75% larger than that of an F8 dwarf.

*HD 117176:* Marcy & Butler (1996) labeled this star as G4 V and the associated radius

for that spectral classification is  $0.92 R_{\odot}$ . However, the measured radius is well over twice that value and it is placed next to HD 10697, a known subgiant, on the color-magnitude diagram.

*HD 190360:* Naef et al. (2003) classified HD 190360 as a G6 IV star and our radius measurement is  $\sim 30\%$  larger than that of a G6 V star. While the star shows no photometric indication of significant evolution off the M-S, the radius measurement is overlarge for a dwarf.

*HD 196885:* This star was labeled as an F8 IV by Jones et al. (2006) and its measured radius exceeds the expected radius for an F8 V by  $\sim 50\%$ . Though there is no photometric evidence of evolution, its radius is significantly larger than expected if the star was a dwarf.

## 5. Conclusion

We observed 24 exoplanet systems in order to measure the host stars' diameters, obtaining 22 limb-darkened angular diameters with errors  $< 15\%$ . After the LD diameters were converted to linear radii when combined with *Hipparcos* parallax, 19 dwarf stars boasted radius errors of  $< 15\%$ , and these were plotted with the radii from the eclipsing binary sample from Andersen (1991). These new results tripled the number of stars in the  $0.5 \leq (B - V) \leq 1.0$  range with known radii. Three giants, 5 subgiants, 11 dwarfs, and 5 moderately evolved stars were measured, covering a wide range of evolutionary stages.

Many thanks to Chris Farrington for his invaluable assistance in obtaining some of the data used here. The CHARA Array is funded by the National Science Foundation through NSF grants AST-0307562 and AST-0606958 and by Georgia State University through the College of Arts and Sciences and the Office of the Vice President for Research. This research has made use of the SIMBAD literature database, operated at CDS, Strasbourg, France, and of NASA's Astrophysics Data System. This publication makes use of data products from the Two Micron All Sky Survey, which is a joint project of the University of Massachusetts and the Infrared Processing and Analysis Center/California Institute of Technology, funded by the National Aeronautics and Space Administration and the National Science Foundation.

## REFERENCES

- Allende Prieto, C., & Lambert, D. L. 1999, A&A, 352, 555

- Andersen, J. 1991, A&A Rev., 3, 91
- Baines, E. K., et al. 2007, ApJ, 661, L195
- Berger, D. H., et al. 2006, ApJ, 644, 475
- Bouchy, F., et al. 2005, A&A, 444, L15
- Butler, R. P., et al. 1997, ApJ, 474, L115
- Butler, R. P., et al. 1999, ApJ, 526, 916
- Butler, R. P. et al. 2003, ApJ, 582, 455
- Butler, R. P., et al. 2006, ApJ, 646, 505
- Claret, A., Diaz-Cordoves, J., & Gimenez, A. 1995, A&AS, 114, 247
- Cochran, W. D., et al. 1997, ApJ, 483, 457
- Cohen, M., Wheaton, W. A., & Megeath, S. T. 2003, AJ, 126, 1090
- Colina, L., Bohlin, R. C., & Castelli, F. 1996, AJ, 112, 307
- Cox, A. N. 2000, Allen's astrophysical quantities, 4th ed., ed. A. N. Cox (New York: AIP Press; Springer)
- Cutri, R. M., et al. 2003, The IRSA 2MASS All-Sky Point Source Catalog, NASA/IPAC Infrared Science Archive
- Farrington, C. D., & McAlister, H. A. 2006, Proc. SPIE, 6268
- Fischer, D. A., et al. 2001, ApJ, 551, 1107
- Fischer, D. A., et al. 2003, ApJ, 590, 1081
- Fischer, D. A., & Valenti, J. 2005, ApJ, 622, 1102
- Girardi, L., Bressan, A., Bertelli, G., & Chiosi, C. 2000, A&AS, 141, 371
- Gray, R. O., Graham, P. W., & Hoyt, S. R. 2001, AJ, 121, 2159
- Gray, R. O., Corbally, C. J., Garrison, R. F., McFadden, M. T., & Robinson, P. E. 2003, AJ, 126, 2048
- Hanbury-Brown, R., et al. 1974, MNRAS, 167, 475

- Johnson, H. L., Iriarte, B., Mitchell, R. I., & Wisniewskj, W. Z. 1966, Communications of the Lunar and Planetary Laboratory, 4, 99
- Jones, B. W., Sleep, P. N., & Underwood, D. R. 2006, ApJ, 649, 1010
- Marcy, G. W., & Butler, R. P. 1996, ApJ, 464, L147
- Marcy, G. W., et al. 1997, ApJ, 481, 926
- Marcy, G. W., et al. 2002, ApJ, 581, 1375
- Marcy, G. W., et al. 2005, ApJ, 619, 570
- Mayor, M., et al. 2004, A&A, 415, 391
- McAlister, H. A., et al. 2005, ApJ, 628, 439
- Mermilliod, J. C. 1997, VizieR Online Data Catalog, 2168, 0
- Monet, D. G., et al. 2003, AJ, 125, 984
- Morel, M., & Magnenat, P. 1978, A&AS, 34, 477
- Myers, J. R., et al. 2002, VizieR Online Data Catalog, 5109, 0
- Naef, D., et al. 2003, A&A, 410, 1051
- Noyes, R. W., et al. 1997, ApJ, 483, L111
- Perrier, C., et al. 2003, A&A, 410, 1039
- Perryman, M. A. C., & ESA 1997, ESA Special Publication, 1200
- Ribas, et al. 2003, A&A, 411, L501
- Santos, N. C., Israelian, G., & Mayor, M. 2004, A&A, 415, 1153
- Sato, B., et al. 2003, ApJ, 597, L157
- Shao, M., & Colavita, M. M. 1992, ARA&A, 30, 457
- Soubiran, C., & Girard, P. 2005, A&A, 438, 139
- Sousa, S. G., et al. 2006, A&A, 458, 873
- Takeda, Y., et al. 2005, PASJ, 57, 109

ten Brummelaar, T. A., et al. 2005, ApJ, 628, 453

Valenti, J. A., & Fischer, D. A. 2005, ApJS, 159, 141

van Leeuwen, F. 2007, Hipparcos, the New Reduction of the Raw Data (Cambridge, UK  
Series: Astrophysics and Space Science Library; Springer)

Vogt, S. S., et al. 2000, ApJ, 536, 902

Table 1. Observing Log.

Target HD	Other Name	Calibrator HD	Baseline (length)	Date (UT)	Number of Observations
3651	54 Psc	4568	S1-E1 (331 m)	2005/10/22	2
				2005/10/24	6
9826	<i>v</i> And	6920	S1-E1 (331 m)	2004/01/14	13
				2004/01/15	6
			W1-S2 (249 m)	2007/09/05	15
10697	109 Psc	10477	S1-E1 (331 m)	2005/10/23	4
				2007/09/13	2
				2007/09/14	4
11964	...	13456	W1-S1 (279 m)	2005/12/13	1
				2005/12/16	5
13189	...	11007	S1-E1 (331 m)	2005/12/12	4
				2006/08/14	4
19994	94 Cet	19411	S1-E1 (331 m)	2005/10/21	4
				2005/10/27	6
				2005/12/10	6
20367	...	21864	S1-E1 (331 m)	2005/12/12	5
				2007/01/24	2
23596	...	22521	S1-E1 (331 m)	2007/09/11	7
				2007/09/14	5
38529	...	43318	S1-E1 (331 m)	2005/10/22	2
				2005/10/24	2
				2005/12/06	8
50554	...	49736	S1-E1 (331 m)	2005/12/07	2
				2005/12/12	5
59686	...	61630	S1-E1 (331 m)	2005/12/06	8
				2007/04/02	9
75732	55 Cnc	72779	S1-E1 (331 m)	2007/03/26	5
				2007/03/30	6
104985	...	97619	E1-W1 (314 m)	2007/04/26	7
				2006/05/20	5
117176	70 Vir	121107	S1-E1 (331 m)	2007/04/02	6
				2007/02/05	10
120136	$\tau$ Boo	121107	S1-E1 (331 m)	2007/03/25	2
				2007/03/26	5
				2007/03/30	8
				2006/05/19	4
143761	$\rho$ CrB	136849	S1-E1 (331 m)	2006/06/09	1
				2006/08/11	3
145675	14 Her	151044	S1-E1 (331 m)	2006/08/12	7
				2006/06/09	1
177830	...	176377	S1-E1 (331 m)	2006/08/13	6
				2006/08/13	6
186427	16 Cyg B	184960	S1-E1 (331 m)	2006/08/13	6
				2007/09/12	6
189733	...	190993	S1-E1 (331 m)	2006/05/31	1

Table 1—Continued

Target HD	Other Name	Calibrator HD	Baseline (length)	Date (UT)	Number of Observations
				2006/06/01	2
				2006/06/08	1
				2006/08/15	5
190228	...	190470	S1-E1 (331 m)	2006/08/14	8
190360	...	189108	S1-E1 (331 m)	2006/06/09	1
				2006/08/11	9
196885	...	194012	S1-E1 (331 m)	2005/10/27	4
				2006/08/14	5
217014	51 Peg A	218261	S1-E1 (331 m)	2006/08/12	7

Note. — Observations for HD 189733 were obtained using the *H*-band while all other observations were obtained using the *K'*-band.

Table 2. Calibrator Stars’ Basic Parameters.

HD	$T_{\text{eff}}$ (K)	$\log g$	$\theta_{\text{LD}}$ (mas)	Ref
4568	6310	3.95	0.347±0.006	1
6920	6026	3.67	0.543±0.028	1
10477	4800	2.24	0.439±0.018	2
11007	6165	4.20	0.511±0.025	1
13456	6760	4.00	0.380±0.011	1
19411	5050	2.54	0.485±0.019	2
21864	4660	2.14	0.440±0.018	2
22521	5783	3.96	0.377±0.008	3
43318	6456	4.01	0.491±0.030	1
49736	6026	4.25	0.312±0.006	1
61630	4400	1.94	1.116±0.067	2
72779	5790	2.90	0.413±0.010	4
97619	4390	1.94	0.835±0.083	2
121107	5450	1.74	0.686±0.013	2
136849	10741	4.24	0.255±0.016	1
151044	6166	4.38	0.379±0.012	1
176377	5888	4.47	0.358±0.007	1
184960	6456	4.33	0.489±0.017	1
189108	4800	2.34	0.585±0.051	2
190470	4968	4.50	0.340±0.009	5
190993	19055	...	0.167±0.035	6
194012	6309	4.36	0.412±0.008	1
218261	6165	4.40	0.384±0.015	1

Note. — References indicate the sources of the  $T_{\text{eff}}$  and  $\log g$  values. (1) Allende Prieto & Lambert (1999); (2) Cox (2000).  $T_{\text{eff}}$  and  $\log g$  based on spectral type as listed in the *SIMBAD Astronomical Database*; (3) Soubiran & Girard (2005); (4) Gray et al. (2001); (5) Gray et al. (2003); (6) Baines et al. (2007)

Table 3. Example of Exoplanet Host Stars’ Calibrated Visibilities.

Target Name	MJD	<i>B</i> (m)	$\Theta$ (deg)	$V_c$	$\sigma V_c$
HD 3651	53665.387	311.95	174.5	0.621	0.072
	53665.400	312.97	171.3	0.647	0.059
	53667.328	312.67	187.9	0.703	0.041
	53667.347	311.52	183.3	0.723	0.059
	53667.364	311.29	179.0	0.676	0.046
	53667.377	311.69	175.7	0.713	0.072
	53667.390	312.53	172.5	0.653	0.053
	53667.402	313.79	169.4	0.590	0.063

Note. — The position angle ( $\Theta$ ) is calculated to be east of north. The complete version of this table is in the electronic edition of the *Astrophysical Journal*. A portion is shown here for guidance regarding its content.

Table 4. Exoplanet Host Stars’ Calibrated Visibilities.

Target Name	MJD	$B$ (m)	$\Theta$ (deg)	$V_c$	$\sigma V_c$
HD 3651	53665.387	311.95	174.5	0.621	0.072
	53665.400	312.97	171.3	0.647	0.059
	53667.328	312.67	187.9	0.703	0.041
	53667.347	311.52	183.3	0.723	0.059
	53667.364	311.29	179.0	0.676	0.046
	53667.377	311.69	175.7	0.713	0.072
	53667.390	312.53	172.5	0.653	0.053
	53667.402	313.79	169.4	0.590	0.063
	HD 9826	53018.136	330.55	190.3	0.366
		53018.146	330.60	188.0	0.366
		53018.154	330.63	186.0	0.362
		53018.165	330.64	183.4	0.403
		53018.180	330.65	269.9	0.387
		53018.190	330.65	177.5	0.415
		53018.200	330.64	175.1	0.373
		53018.211	330.61	172.6	0.395
		53018.221	330.56	170.2	0.355
		53018.233	330.45	167.4	0.364
		53018.244	330.28	164.9	0.403
		53018.254	330.05	162.7	0.427
		53018.263	329.73	160.6	0.346
		53019.175	330.65	180.5	0.337
		53019.186	330.65	177.9	0.343
		53019.196	330.64	175.5	0.387
		53019.207	330.62	172.9	0.370
		53019.216	330.57	170.6	0.329
		53019.255	329.93	161.8	0.347
	54348.292	242.92	177.3	0.483	0.077
	54348.302	243.11	174.3	0.529	0.058

Table 4—Continued

Target Name	MJD	<i>B</i> (m)	$\Theta$ (deg)	$V_c$	$\sigma V_c$
	54348.311	243.43	171.4	0.537	0.050
	54348.322	243.88	168.4	0.563	0.071
	54348.334	244.57	164.7	0.608	0.060
	54348.344	245.24	161.7	0.649	0.060
	54348.355	245.98	158.7	0.630	0.062
	54348.366	246.73	155.7	0.610	0.054
	54348.376	247.46	152.8	0.558	0.044
	54348.397	248.67	147.4	0.577	0.046
	54348.408	249.12	144.6	0.615	0.050
	54348.419	249.36	141.9	0.618	0.054
	54348.435	249.26	138.2	0.721	0.085
	54348.456	248.12	133.5	0.652	0.093
	54348.467	246.94	131.0	0.579	0.074
HD 10697	53666.427	309.50	175.2	1.043	0.090
	53666.443	310.79	171.2	0.928	0.068
	53666.456	312.37	167.9	1.004	0.104
	53666.470	314.46	164.6	0.832	0.075
	54356.765	317.17	226.9	0.883	0.103
	54356.775	320.54	227.4	1.029	0.125
	54357.783	323.64	228.1	0.851	0.077
	54357.792	325.84	228.8	0.723	0.068
	54357.802	327.87	229.7	0.816	0.089
	54357.810	328.95	230.4	0.791	0.061
HD 11964	53717.253	269.16	127.2	0.903	0.080
	53720.237	266.29	127.2	0.839	0.085
	53720.252	271.34	127.3	0.834	0.089
	53720.264	274.76	127.5	0.770	0.088
	53720.279	277.28	128.1	0.843	0.137
	53720.295	278.45	128.9	0.864	0.156

Table 4—Continued

Target Name	MJD	<i>B</i> (m)	$\Theta$ (deg)	$V_c$	$\sigma V_c$
HD 13189	53716.270	327.09	184.4	0.607	0.056
	53716.285	326.91	180.9	0.531	0.081
	53716.298	326.96	177.7	0.589	0.095
	53716.312	327.21	174.3	0.575	0.130
	53961.441	326.60	216.4	0.622	0.051
	53961.454	328.41	214.4	0.648	0.062
	53961.467	329.65	212.2	0.643	0.073
	53961.481	330.38	209.8	0.607	0.040
HD 19994	53664.336	297.29	213.9	0.588	0.068
	53664.352	288.97	211.5	0.736	0.073
	53664.365	281.76	209.1	0.669	0.056
	53664.378	274.84	206.6	0.598	0.062
	53670.286	312.83	217.7	0.750	0.080
	53670.301	306.26	216.2	0.726	0.084
	53670.316	298.87	214.4	0.690	0.055
	53670.333	290.10	211.9	0.764	0.076
	53670.350	281.33	209.0	0.706	0.050
	53670.367	272.38	205.5	0.792	0.048
	53714.182	305.88	216.1	0.712	0.083
	53714.208	292.79	212.7	0.795	0.107
	53714.220	286.27	210.7	0.787	0.078
	53714.239	276.58	207.2	0.713	0.069
HD 20367	53714.254	268.97	204.0	0.775	0.068
	53714.266	262.95	201.0	0.832	0.096
	53716.339	325.81	179.2	0.855	0.147
	53716.353	326.00	175.8	0.934	0.162
	53716.367	326.40	172.6	0.879	0.118
HD 20367	53716.380	326.96	169.5	0.925	0.124
	53716.393	327.66	166.4	0.822	0.174

Table 4—Continued

Target Name	MJD	<i>B</i> (m)	$\Theta$ (deg)	$V_c$	$\sigma V_c$
HD 23596	54124.220	325.80	270.0	0.905	0.138
	54124.232	325.91	176.9	0.919	0.131
	54354.937	317.98	233.5	0.856	0.073
	54354.945	319.79	234.9	0.929	0.080
	54354.953	321.52	236.4	0.967	0.068
	54354.960	322.96	237.9	0.915	0.074
	54354.969	324.30	239.5	0.879	0.056
	54354.977	325.43	241.2	0.826	0.060
	54354.985	326.44	242.9	0.818	0.057
	54357.938	320.98	234.3	1.040	0.098
HD 38529	54357.954	324.23	237.3	0.968	0.077
	54357.960	325.22	238.5	0.964	0.108
	54357.967	326.10	239.7	0.972	0.059
	54357.973	326.90	241.0	0.945	0.068
	53665.444	299.99	212.7	0.809	0.072
	53665.457	293.81	210.6	0.866	0.101
	53667.451	294.20	210.8	0.879	0.239
	53667.464	287.73	208.4	0.801	0.085
	53710.300	309.43	215.5	0.889	0.086
	53710.314	303.46	213.7	0.823	0.103
HD 50554	53710.330	295.80	211.3	0.805	0.089
	53710.344	289.03	208.9	0.726	0.105
	53710.357	282.66	206.4	0.808	0.081
	53710.370	276.44	203.6	0.888	0.065
	53710.384	270.21	200.2	0.895	0.087
	53710.397	265.22	196.9	0.902	0.083
	53711.523	317.33	174.2	0.874	0.127
	53711.537	318.32	170.7	0.783	0.090
	53716.422	321.04	195.4	1.006	0.138

Table 4—Continued

Target Name	MJD	<i>B</i> (m)	$\Theta$ (deg)	$V_c$	$\sigma V_c$
HD 59686	53716.435	319.48	192.2	0.905	0.091
	53716.449	318.20	189.0	0.984	0.083
	53716.463	317.30	185.7	1.027	0.096
	53716.479	316.73	181.7	0.956	0.150
	53710.430	316.56	203.4	0.406	0.038
	53710.445	313.18	200.3	0.411	0.046
	53710.460	309.92	196.8	0.410	0.055
	53710.474	307.34	193.6	0.420	0.061
	53710.487	305.25	190.4	0.440	0.045
	53710.501	303.69	187.0	0.435	0.032
	53710.514	302.71	183.6	0.453	0.044
	53710.527	302.35	90.2	0.446	0.037
	54192.202	302.46	182.1	0.458	0.038
	54192.223	302.65	176.6	0.490	0.039
	54192.235	303.49	173.5	0.448	0.035
HD 75732	54192.246	304.67	170.7	0.465	0.051
	54192.257	306.19	168.1	0.451	0.042
	54192.268	307.97	165.5	0.462	0.032
	54192.279	310.10	163.0	0.447	0.030
	54192.290	312.37	160.5	0.439	0.027
	54192.300	314.78	158.2	0.445	0.022
	54185.221	325.59	195.2	0.562	0.061
	54185.234	324.51	192.1	0.579	0.065
	54185.304	322.77	175.4	0.568	0.054
	54185.317	323.32	172.3	0.576	0.058
	54185.330	324.09	169.2	0.527	0.038
	54189.207	325.83	195.9	0.730	0.079
	54189.221	324.70	192.7	0.651	0.090
	54189.235	323.75	189.5	0.743	0.078

Table 4—Continued

Target Name	MJD	<i>B</i> (m)	$\Theta$ (deg)	$V_c$	$\sigma V_c$
HD 104985	54189.249	323.02	186.2	0.660	0.078
	54189.264	322.56	182.6	0.765	0.080
	54189.278	322.47	179.1	0.625	0.079
	54216.214	304.67	266.0	0.456	0.045
	54216.249	307.95	253.8	0.525	0.046
	54216.281	310.19	242.6	0.539	0.053
	54216.299	311.13	236.3	0.485	0.051
	54216.315	311.80	230.7	0.477	0.056
	54216.326	312.13	227.2	0.489	0.040
HD 117176	54216.336	312.43	223.6	0.498	0.045
	53875.270	300.08	194.0	0.546	0.061
	53875.292	296.28	188.4	0.538	0.078
	53875.316	294.27	182.2	0.599	0.073
	53875.335	294.34	177.3	0.568	0.058
	53875.352	295.80	172.6	0.571	0.056
	54192.359	311.20	203.9	0.680	0.069
	54192.370	308.00	201.5	0.572	0.079
	54192.383	304.58	198.6	0.629	0.073
HD 120136	54192.429	295.83	187.5	0.469	0.048
	54192.440	294.74	184.6	0.486	0.051
	54192.450	294.20	181.7	0.492	0.041
	54136.370	321.01	222.5	0.629	0.055
	54136.381	324.27	221.9	0.661	0.058
	54136.391	326.49	221.3	0.651	0.063
	54136.400	328.20	220.6	0.633	0.052
	54136.411	329.58	219.8	0.680	0.047
	54136.423	330.44	218.7	0.649	0.060
HD 120136	54136.434	330.67	217.6	0.649	0.044
	54136.445	330.34	216.3	0.605	0.046

Table 4—Continued

Target Name	MJD	<i>B</i> (m)	$\Theta$ (deg)	$V_c$	$\sigma V_c$
54136	54136.456	329.54	214.9	0.630	0.044
	54136.466	328.37	213.5	0.631	0.051
	54184.452	305.95	190.2	0.695	0.076
	54184.470	304.03	185.5	0.668	0.064
	54185.359	323.92	209.3	0.745	0.078
	54185.370	321.72	207.4	0.718	0.050
	54185.382	319.17	205.2	0.735	0.066
	54185.393	316.66	202.9	0.628	0.048
	54185.403	314.46	200.9	0.580	0.057
	54189.375	318.31	204.4	0.656	0.087
	54189.391	314.63	201.0	0.683	0.088
	54189.403	312.13	198.5	0.681	0.055
	54189.413	310.24	196.4	0.736	0.074
	54189.422	308.31	193.9	0.679	0.083
	54189.435	306.50	191.1	0.661	0.079
HD 143761	54189.444	305.25	188.8	0.651	0.069
	54189.455	304.17	186.0	0.624	0.073
	53874.389	328.56	190.3	0.692	0.061
	53874.409	327.99	185.8	0.718	0.079
	53874.425	327.74	181.8	0.790	0.088
HD 145675	53874.444	327.78	177.3	0.884	0.096
	53895.224	329.09	212.5	0.658	0.056
	53958.259	329.81	168.4	0.902	0.054
	53958.275	329.38	164.9	0.878	0.045
	53958.292	328.62	161.0	0.859	0.051
53959	53959.168	329.99	189.3	1.096	0.123
	53959.184	330.18	185.5	1.000	0.089
	53959.200	330.26	181.8	0.964	0.069
	53959.215	330.26	178.1	0.990	0.070

Table 4—Continued

Target Name	MJD	<i>B</i> (m)	$\Theta$ (deg)	$V_c$	$\sigma V_c$
HD 177830	53959.231	330.18	174.5	0.940	0.078
	53959.246	330.01	170.9	0.954	0.067
	53959.261	329.70	167.4	0.808	0.064
	53895.335	330.37	215.0	0.873	0.080
	53960.191	330.06	209.5	0.897	0.074
	53960.208	328.87	206.5	0.886	0.069
	53960.223	327.38	203.5	0.949	0.086
	53960.240	325.46	199.9	0.740	0.097
	53960.259	323.36	195.8	0.705	0.097
	53960.276	321.74	192.0	0.935	0.104
HD 186427	53960.308	325.22	190.2	0.838	0.129
	53960.324	325.76	186.5	0.974	0.092
	53960.337	326.01	183.3	0.981	0.111
	53960.350	326.10	90.2	0.854	0.113
	53960.363	326.03	177.0	0.895	0.090
	53960.377	325.77	173.7	1.035	0.087
	54355.661	319.02	244.1	0.810	0.074
	54355.667	319.87	245.4	0.828	0.090
	54355.673	320.66	246.8	0.828	0.079
	54355.685	322.09	249.5	0.844	0.113
HD 189733	54355.692	322.70	251.0	0.952	0.117
	54355.698	323.25	252.4	0.848	0.113
	53886.905	330.5	...	0.851	0.071
	53887.936	327.9	...	0.843	0.056
	53887.958	324.9	...	0.857	0.054
	53894.865	330.5	...	0.869	0.034
	53962.742	326.5	...	0.909	0.069
HD 209458	53962.761	323.8	...	0.863	0.049
	53962.778	321.3	...	0.877	0.045

Table 4—Continued

Target Name	MJD	<i>B</i> (m)	$\Theta$ (deg)	$V_c$	$\sigma V_c$
HD 190228	53962.793	319.0	...	0.839	0.045
	53962.824	315.5	...	0.829	0.061
	53961.239	330.20	207.4	0.886	0.043
	53961.253	329.42	204.8	0.882	0.061
	53961.268	328.30	201.8	0.868	0.073
	53961.282	327.09	198.8	0.920	0.106
	53961.299	325.69	195.2	0.814	0.082
	53961.313	324.58	191.9	0.858	0.084
	53961.328	323.60	188.3	0.809	0.080
	53961.346	322.86	184.1	0.933	0.108
HD 190360	53895.487	326.62	193.4	0.754	0.049
	53958.341	325.15	187.2	0.728	0.034
	53958.357	324.67	183.6	0.741	0.035
	53958.372	324.51	269.8	0.741	0.037
	53958.388	324.72	176.0	0.786	0.056
	53958.405	325.30	172.0	0.698	0.039
	53958.421	326.15	168.2	0.657	0.052
	53958.436	327.17	164.7	0.670	0.068
	53958.451	328.17	161.6	0.636	0.060
	53958.465	329.11	158.6	0.673	0.043
HD 196885	53670.153	289.70	188.8	0.909	0.085
	53670.169	287.85	184.6	0.783	0.075
	53670.183	287.18	180.7	0.848	0.071
	53670.196	287.44	177.1	0.950	0.090
	53961.161	330.09	220.6	0.850	0.077
	53961.175	330.66	219.7	0.898	0.077
	53961.188	330.30	218.8	0.819	0.085
	53961.201	329.05	217.5	0.926	0.063
	53961.214	327.15	216.2	0.774	0.065

Table 4—Continued

Target Name	MJD	<i>B</i> (m)	$\Theta$ (deg)	$V_c$	$\sigma V_c$
HD 217014	53959.290	329.68	218.7	0.677	0.070
	53959.303	330.50	217.2	0.696	0.059
	53959.316	330.63	215.6	0.639	0.061
	53959.329	330.08	213.7	0.656	0.037
	53959.343	328.87	211.6	0.699	0.049
	53959.357	327.11	209.3	0.611	0.074
	53959.372	324.94	206.7	0.713	0.056

Table 5. Photometric Sources.

HD	<i>U</i>	<i>B</i>	<i>V</i>	<i>R</i>	<i>I</i>
3651	1	1	1	1	1
9826	1	1	1	1	1
10697	...	2	2	3	3
11964	...	2	2	3	3
13189	...	2	2	3	3
19994	4	4	4	3	3
20367	...	2	2	3	3
23596	...	2	2	3	3
38529	...	2	2	3	3
50554	...	2	2	3	3
59686	...	2	2	3	3
75732	...	2	2	3	3
104985	4	4	4	3	3
117176	1	1	1	1	1
120136	1	1	1	1	1
143761	4	4	4	3	3
145675	...	2	2	3	3
177830	5	5	5	3	3
186427	4	4	4	3	3
189733	...	2	2	3	3
190228	6	6	6	3	3
190360	4	4	4	3	3
196885	...	2	2	3	3
217014	1	1	1	1	1

Note. — All *JHK* photometry were from Cutri et al. (2003). Sources:  
(1) Morel & Magnenat (1978);  
(2) Perryman & ESA (1997); (3)  
Monet et al. (2003); (4) Johnson et al.  
(1966); (5) 1997yCat.2168....0M; (6)  
Myers et al. (2002)

Table 6. Exoplanet Host Star Angular Diameter Measurements.

HD	Spectral Type	$T_{\text{eff}}$ (K)	$\log g$	$\mu_\lambda$	$\pi$ (mas)	$\theta_{\text{SED}}$ (mas)	$\theta_{\text{UD}}$ (mas)	$\theta_{\text{LD}}$ (mas)	$\sigma_{\text{LD}}$ (%)	$R_{\text{linear}}$ ( $R_\odot$ )	$\sigma_R$ (%)	$R_{\text{standard}}$ ( $R_\odot$ )
3651	K0 V	5173	4.37	0.28	$90.43 \pm 0.32$	$0.767 \pm 0.078$	$0.773 \pm 0.026$	$0.790 \pm 0.027$	3	$0.947 \pm 0.032$	3	0.85
9826	F8 V	6212	4.26	0.24	$74.14 \pm 0.19$	$1.095 \pm 0.032$	$1.091 \pm 0.009$	$1.114 \pm 0.009$	1	$1.631 \pm 0.014$	1	1.2
10697	G5 IV	5641	4.05	0.28	$30.69 \pm 0.43$	$0.496 \pm 0.015$	$0.475 \pm 0.046$	$0.485 \pm 0.046$	9	$1.72 \pm 0.17$	10	0.92
11964	G5	5248 <sup>a</sup>	3.82 <sup>a</sup>	0.30	$30.43 \pm 0.60$	$0.553 \pm 0.013$	$0.597 \pm 0.078$	$0.611 \pm 0.081$	13	$2.18 \pm 0.29$	13	0.92
13189	K2 II	4050 <sup>b</sup>	1.74 <sup>b</sup>	0.37	$1.80 \pm 0.73$	$0.783 \pm 0.043$	$0.811 \pm 0.027$	$0.836 \pm 0.028$	3	$50.39 \pm 20.51$	41	$\sim 20$
19994	F8 V	6217	4.29	0.24	$44.28 \pm 0.28$	$0.693 \pm 0.025$	$0.774 \pm 0.026$	$0.788 \pm 0.026$	3	$1.930 \pm 0.067$	3	1.2
20367	G0 V	6138	4.53	0.25	$37.48 \pm 0.63$	$0.386 \pm 0.014$	$0.400 \pm 0.107$	$0.408 \pm 0.109$	27	$1.18 \pm 0.32$	27	1.1
23596	F8	6108	4.25	0.25	$19.84 \pm 0.49$	$0.264 \pm 0.008$	$0.374 \pm 0.043$	$0.381 \pm 0.044$	12	$2.09 \pm 0.24$	12	1.2
38529	G4 IV	5674	3.94	0.28	$25.46 \pm 0.40$	$0.570 \pm 0.028$	$0.561 \pm 0.048$	$0.573 \pm 0.049$	9	$2.44 \pm 0.22$	9	1.1
50554	F8	6026	4.41	0.26	$33.44 \pm 0.59$	$0.326 \pm 0.009$	$0.338 \pm 0.098$	$0.344 \pm 0.100$	29	$1.11 \pm 0.33$	29	1.2
59686	K2 III	4571 <sup>a</sup>	2.40 <sup>a</sup>	0.34	$10.33 \pm 0.28$	$1.287 \pm 0.064$	$1.074 \pm 0.011$	$1.106 \pm 0.011$	1	$11.62 \pm 0.34$	3	$\sim 20$
75732	G8 V	5279	4.37	0.30	$80.55 \pm 0.70$	$0.666 \pm 0.029$	$0.834 \pm 0.024$	$0.854 \pm 0.024$	3	$1.150 \pm 0.035$	3	0.90
104985	G9 III	4877 <sup>c</sup>	2.85 <sup>c</sup>	0.31	$10.30 \pm 0.25$	$0.955 \pm 0.065$	$1.006 \pm 0.022$	$1.032 \pm 0.023$	2	$10.87 \pm 0.36$	3	$\sim 14$
117176	G4 V	5560	4.07	0.28	$55.59 \pm 0.24$	$0.951 \pm 0.068$	$0.986 \pm 0.023$	$1.009 \pm 0.024$	2	$1.968 \pm 0.047$	2	0.92
120136	F7 V	6339	4.19	0.24	$64.03 \pm 0.20$	$0.853 \pm 0.037$	$0.771 \pm 0.015$	$0.786 \pm 0.016$	2	$1.331 \pm 0.027$	2	1.3
143761	G0 V	5853	4.41	0.26	$58.02 \pm 0.28$	$0.700 \pm 0.049$	$0.673 \pm 0.043$	$0.686 \pm 0.044$	6	$1.284 \pm 0.082$	6	1.1
145675	K0 V	5311	4.42	0.30	$56.89 \pm 0.35$	$0.498 \pm 0.008$	$0.363 \pm 0.043$	$0.371 \pm 0.044$	12	$0.708 \pm 0.085$	12	0.85
177830	K0 IV	4804	3.57	0.33	$16.94 \pm 0.63$	$0.515 \pm 0.023$	$0.455 \pm 0.057$	$0.467 \pm 0.058$	12	$2.99 \pm 0.39$	13	0.85
186427	G2.5 V	5772	4.40	0.27	$47.13 \pm 0.27$	$0.494 \pm 0.019$	$0.417 \pm 0.055$	$0.426 \pm 0.056$	13	$0.98 \pm 0.13$	13	1.0
189733	K1 V	5051 <sup>d</sup>	4.53 <sup>d</sup>	0.36	$51.40 \pm 0.69$	$0.363 \pm 0.011$	$0.366 \pm 0.024$	$0.377 \pm 0.024$	6	$0.788 \pm 0.051$	7	0.80
190228	G5 IV	5312	3.87	0.30	$16.25 \pm 0.64$	$0.375 \pm 0.032$	$0.443 \pm 0.045$	$0.453 \pm 0.046$	10	$3.02 \pm 0.33$	11	0.92
190360	G6 IV	5584	4.37	0.28	$63.07 \pm 0.34$	$0.658 \pm 0.031$	$0.682 \pm 0.019$	$0.698 \pm 0.019$	3	$1.200 \pm 0.033$	3	0.92
196885	F8 IV	6310 <sup>a</sup>	4.32 <sup>a</sup>	0.24	$29.83 \pm 0.48$	$0.365 \pm 0.016$	$0.485 \pm 0.046$	$0.494 \pm 0.046$	9	$1.79 \pm 0.17$	10	1.2
217014	G2-3 V	5804	4.42	0.27	$64.09 \pm 0.38$	$0.665 \pm 0.047$	$0.733 \pm 0.026$	$0.748 \pm 0.027$	4	$1.266 \pm 0.046$	4	1.0

| 26 |

Note. — All  $T_{\text{eff}}$  and  $\log g$  are from Santos et al. (2004) unless otherwise noted.

<sup>a</sup>Allende Prieto & Lambert (1999); <sup>b</sup>Cox (2000); <sup>c</sup>Takeda et al. (2005); <sup>d</sup>Sousa et al. (2006)

$\mu_\lambda$  values are from Claret et al. (1995) and  $\pi$  values are from van Leeuwen (2007).

The spectral classes are from the following sources: HD 3651: Fischer et al. (2003); HD 9826: Butler et al. (1999); HD 10697: Vogt et al. (2000); HD 11964: Butler et al. (2006); HD 19994: Mayor et al. (2004); HD 20367: Butler et al. (2006); HD 23596: Valenti & Fischer (2005); HD 38526: Fischer et al. (2001); HD 50554: Perrier et al. (2003); HD 59686: Cox (2000); HD 75732: Marcy et al. (2002); HD 104985: Sato et al. (2003); HD 117176: Marcy & Butler (1996); HD 120136: Butler et al. (1997); HD 143761: Noyes et al. (1997); HD 145675: Butler et al. (2003); HD 177830:

Vogt et al. (2000); HD 186427: Cochran et al. (1997); HD 189733: Bouchy et al. (2005); HD 190228: Perrier et al. (2003); HD 190360: Naef et al. (2003); HD 196885: Jones et al. (2006); and HD 217014: Marcy et al. (1997).

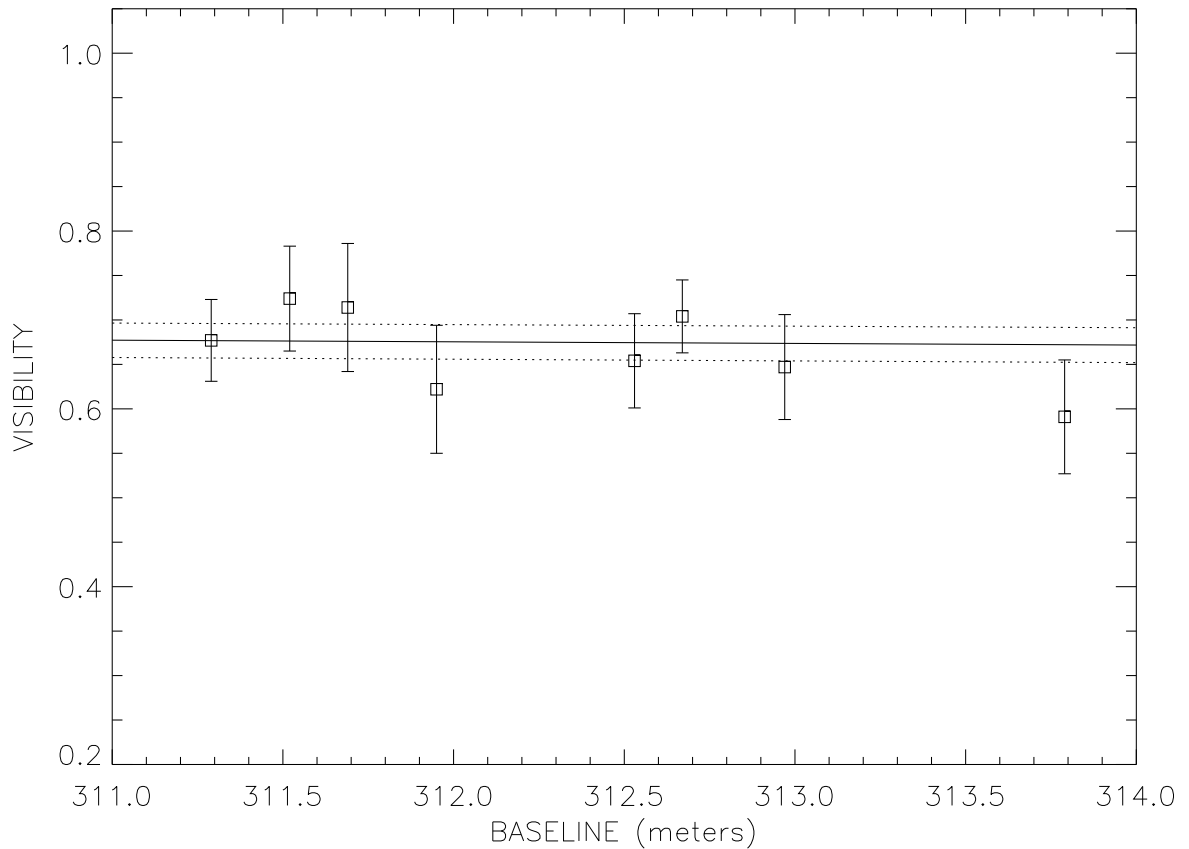


Fig. 1.— Example LD disk diameter fit. HD 3651: Calibrated visibility vs. baseline. The solid line represents the theoretical visibility curve for a star with the best fit  $\theta_{\text{LD}}$ , the dashed lines are the  $1\sigma$  error limits of the diameter fit, the  $\square$ s are the calibrated visibilities, and the vertical lines are the measured errors. [See the electronic edition of the *Astrophysical Journal* for Figures 2-24.]

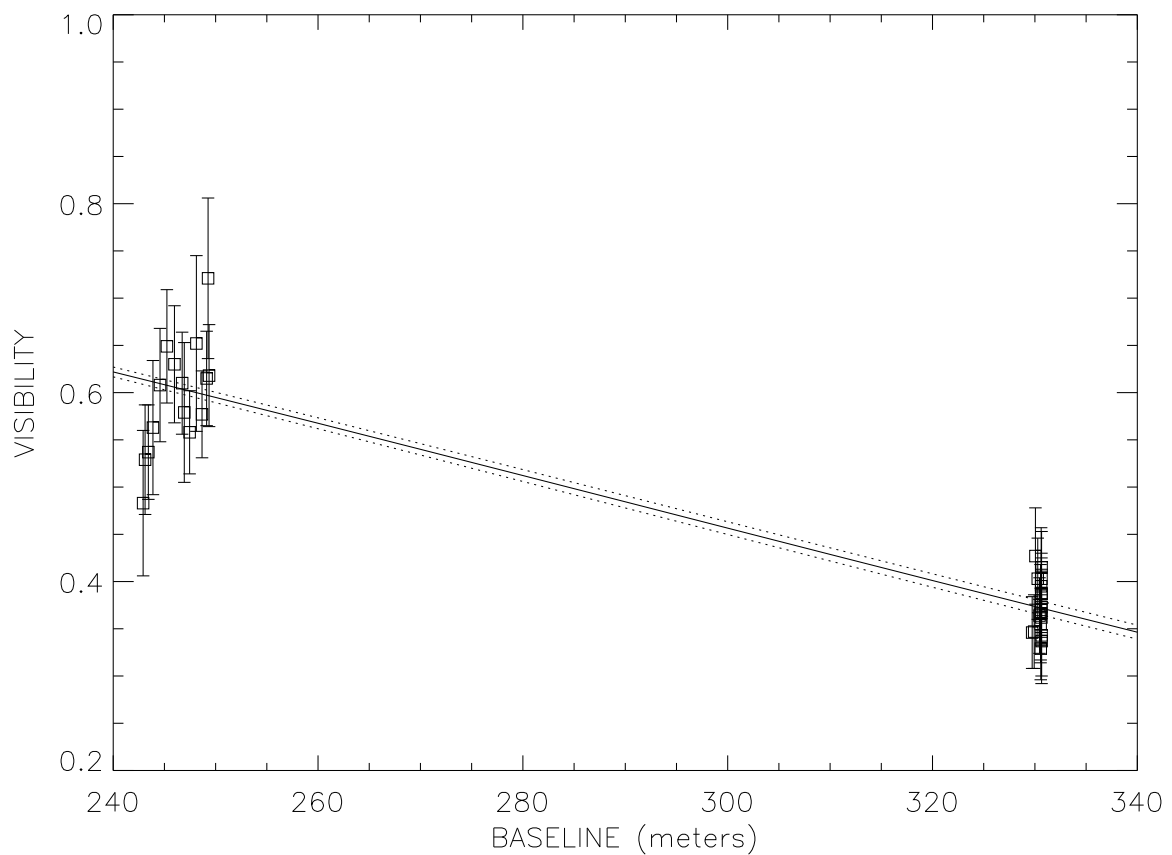


Fig. 2.— HD 9826 limb-darkened disk diameter fit.

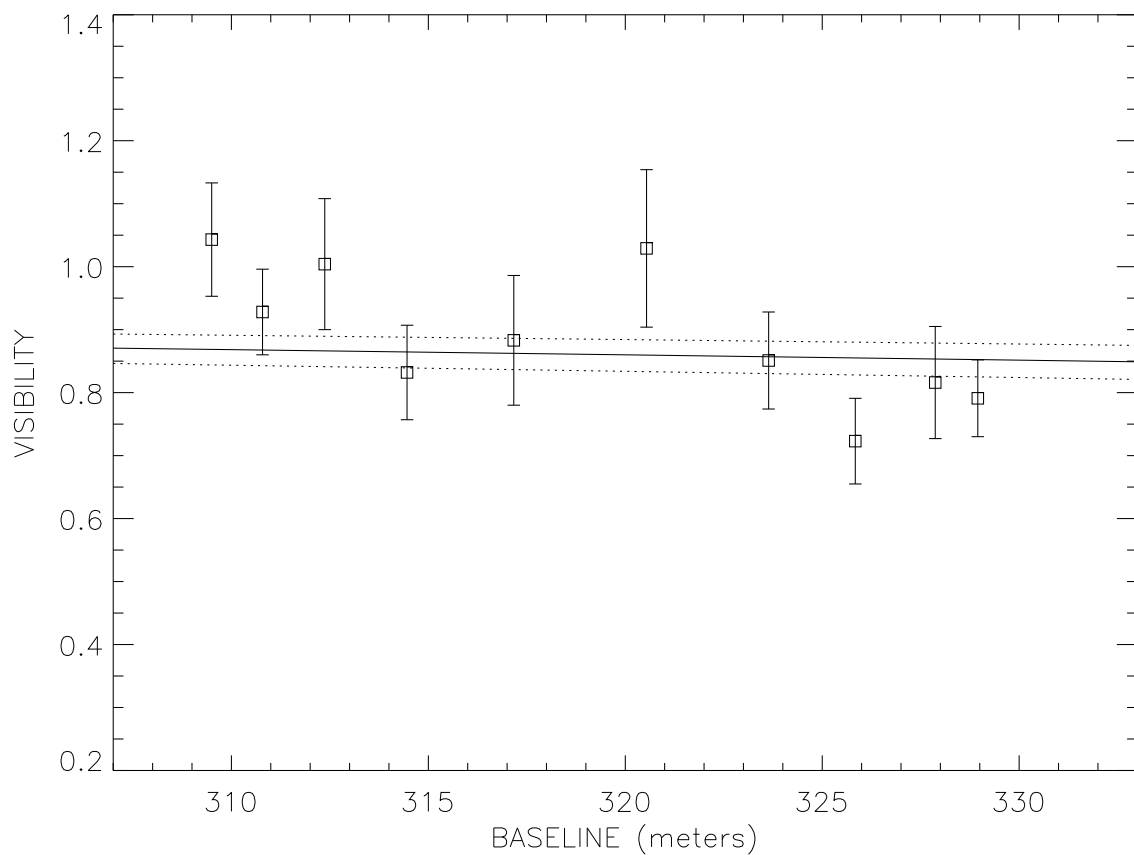


Fig. 3.— HD 10697 limb-darkened disk diameter fit.

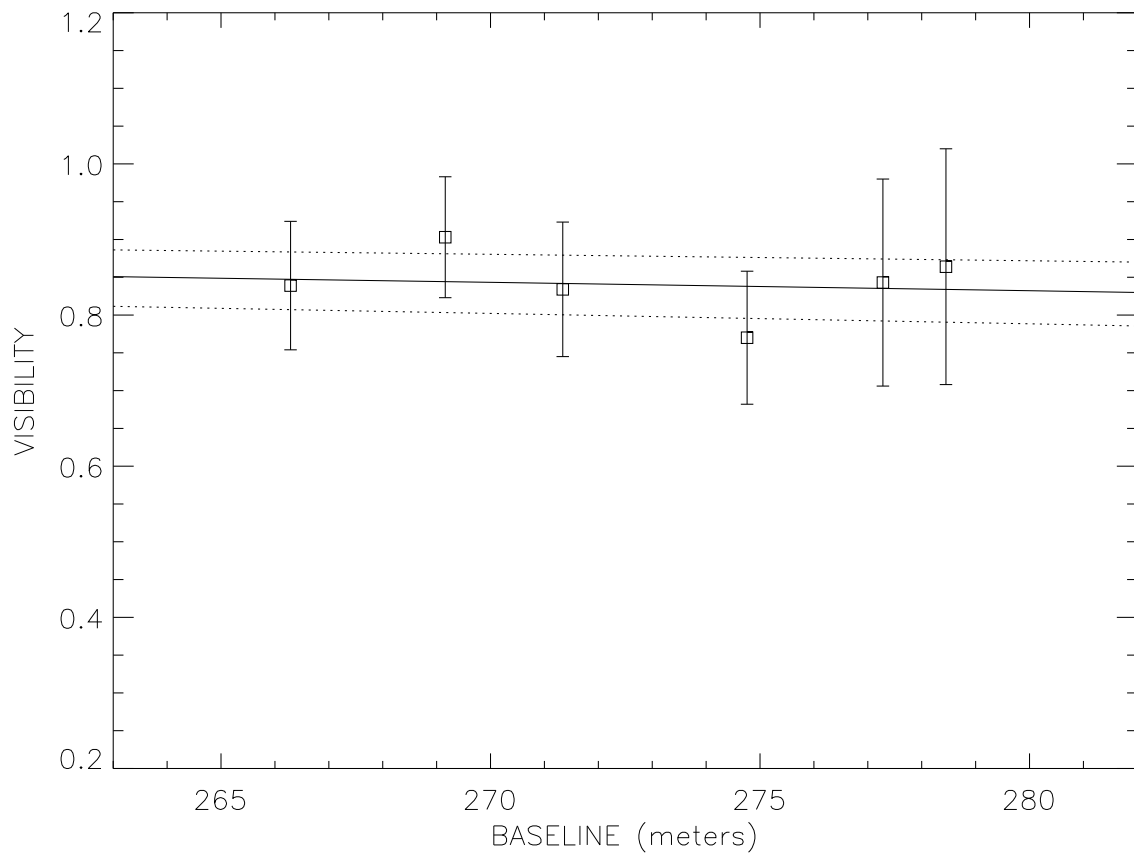


Fig. 4.— HD 11964 limb-darkened disk diameter fit.

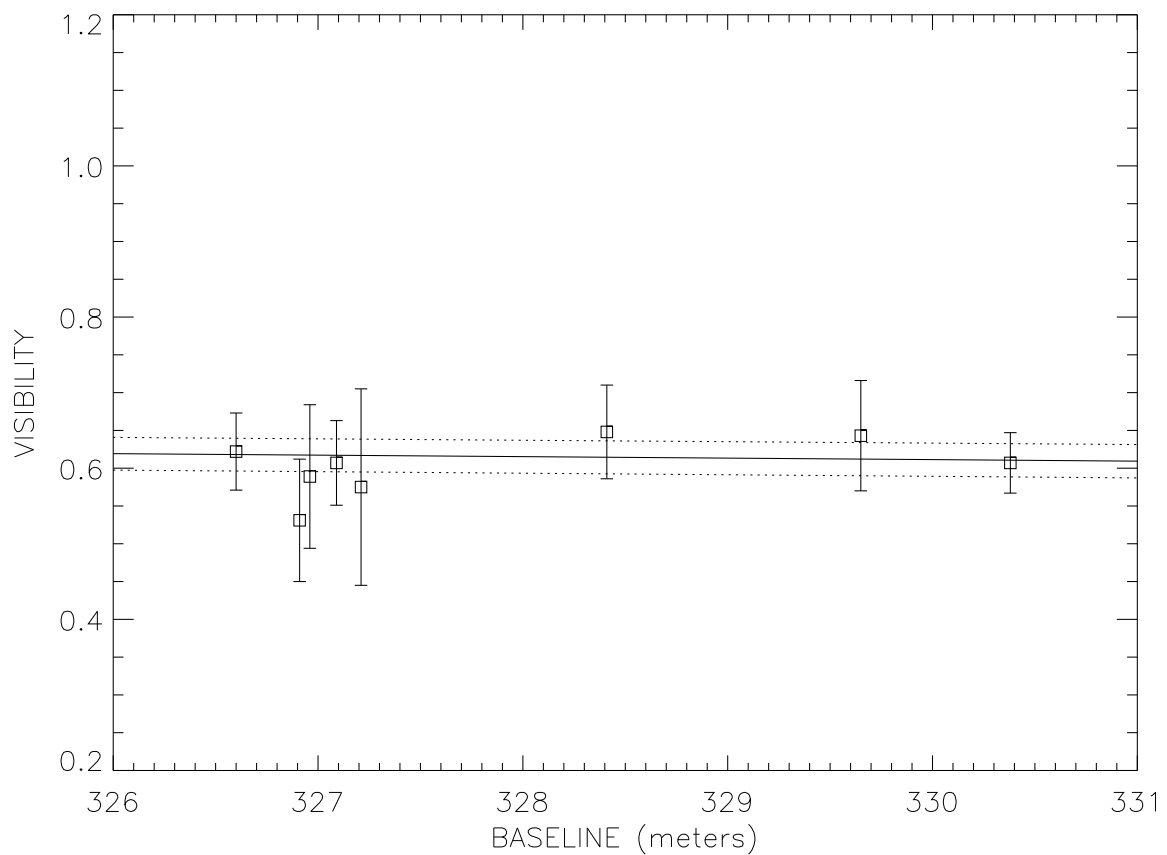


Fig. 5.— HD 13189 limb-darkened disk diameter fit.

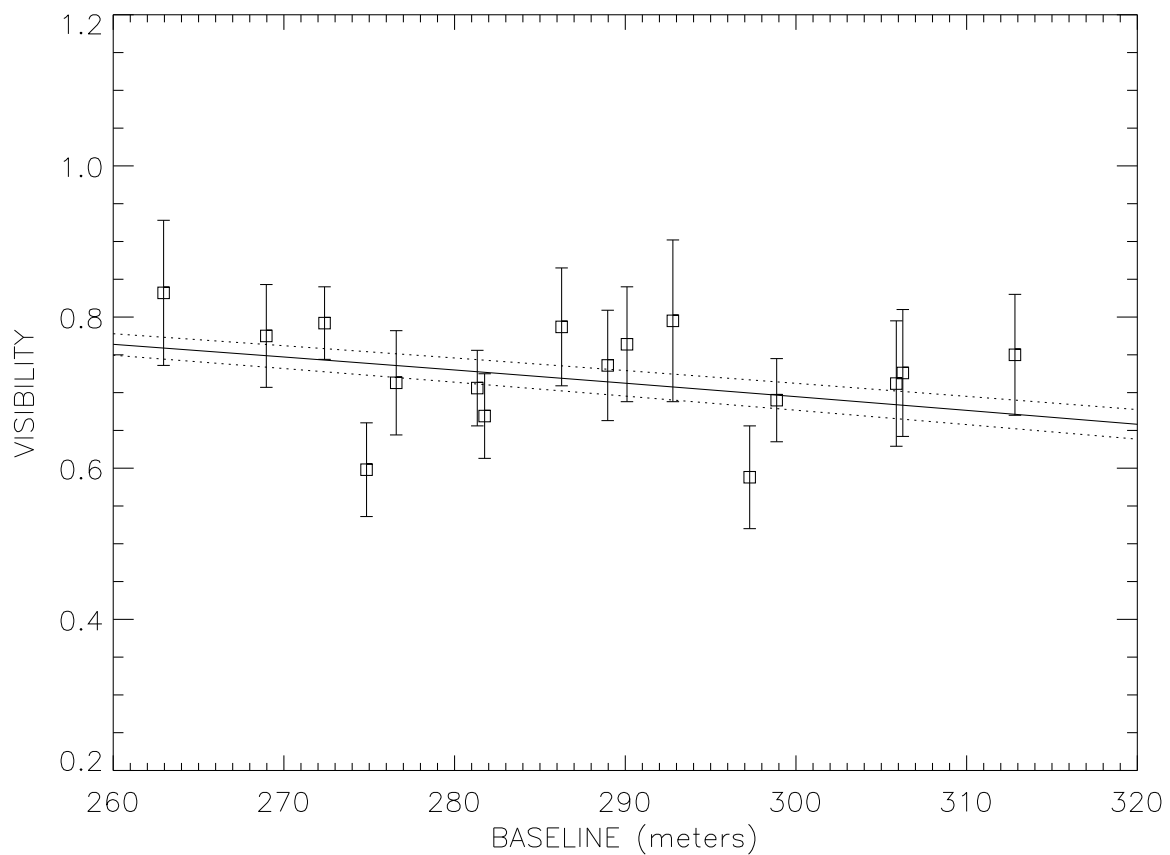


Fig. 6.— HD 19994 limb-darkened disk diameter fit.

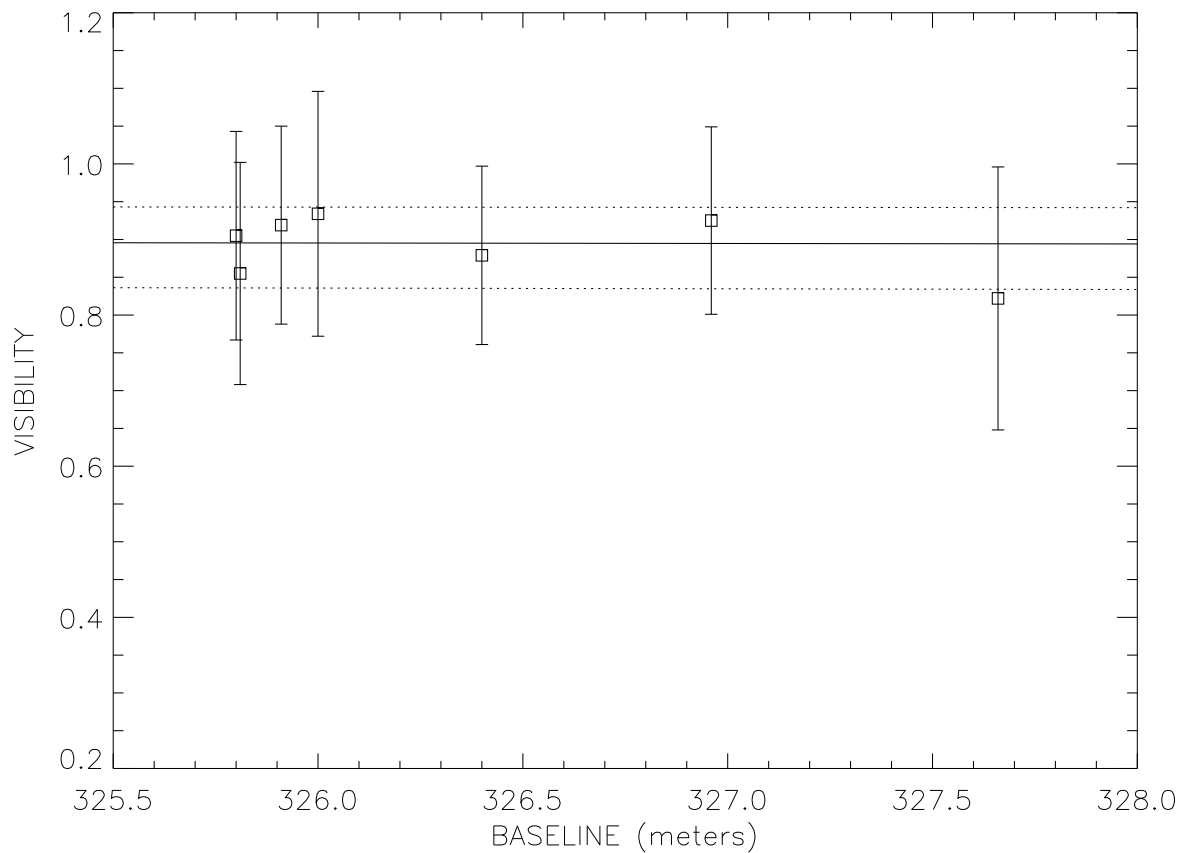


Fig. 7.— HD 20367 limb-darkened disk diameter fit.

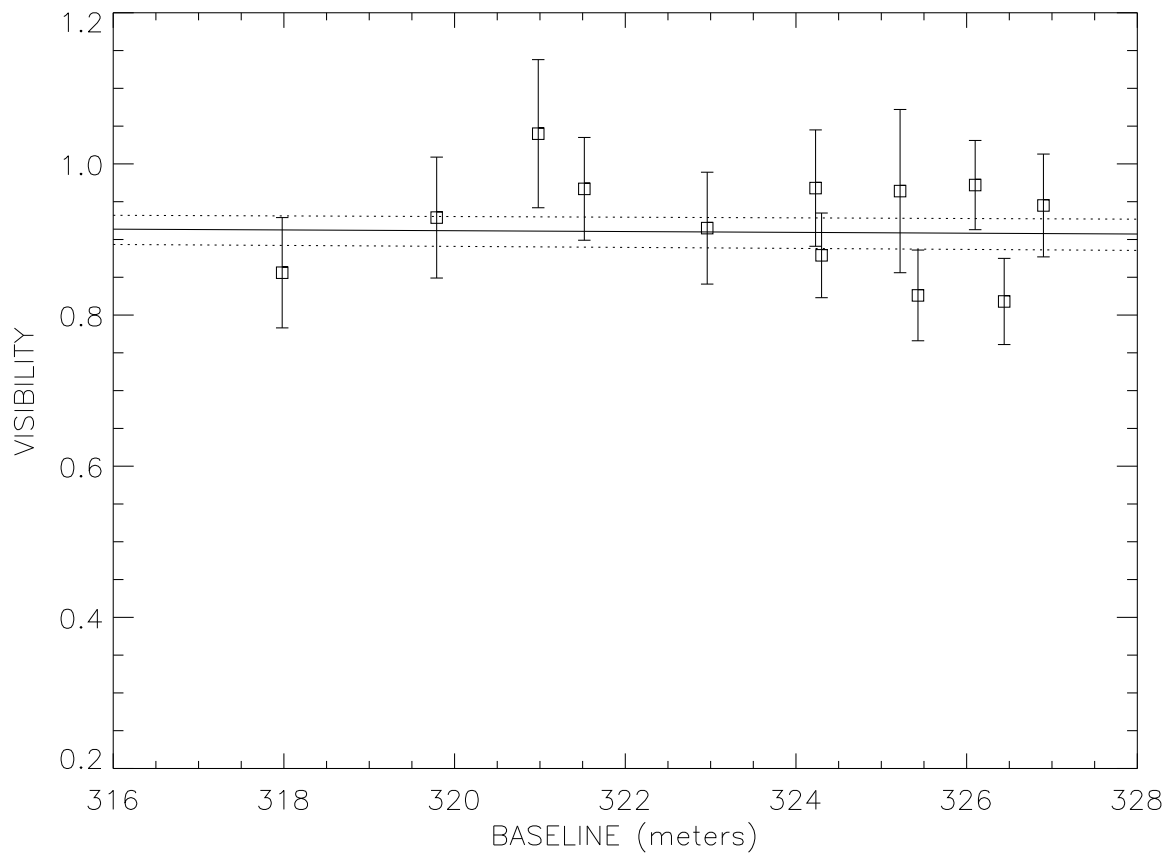


Fig. 8.— HD 23596 limb-darkened disk diameter fit.

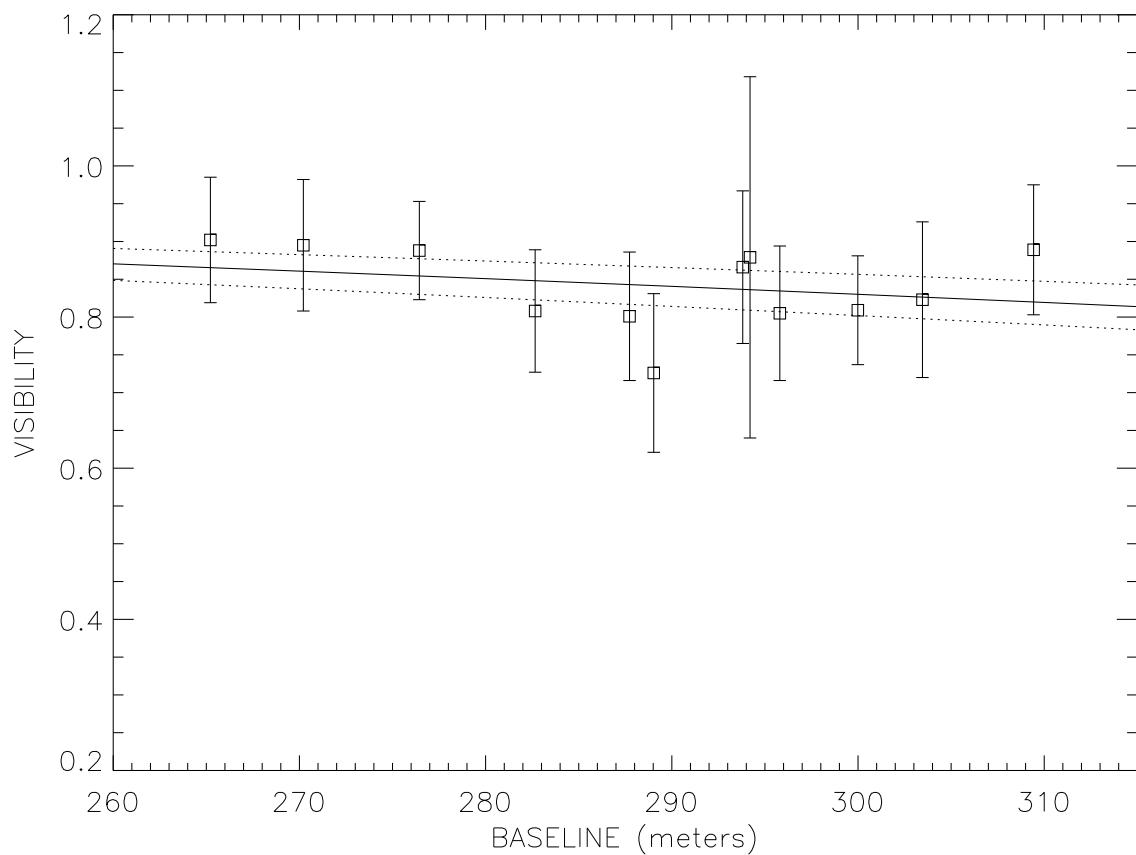


Fig. 9.— HD 38529 limb-darkened disk diameter fit.

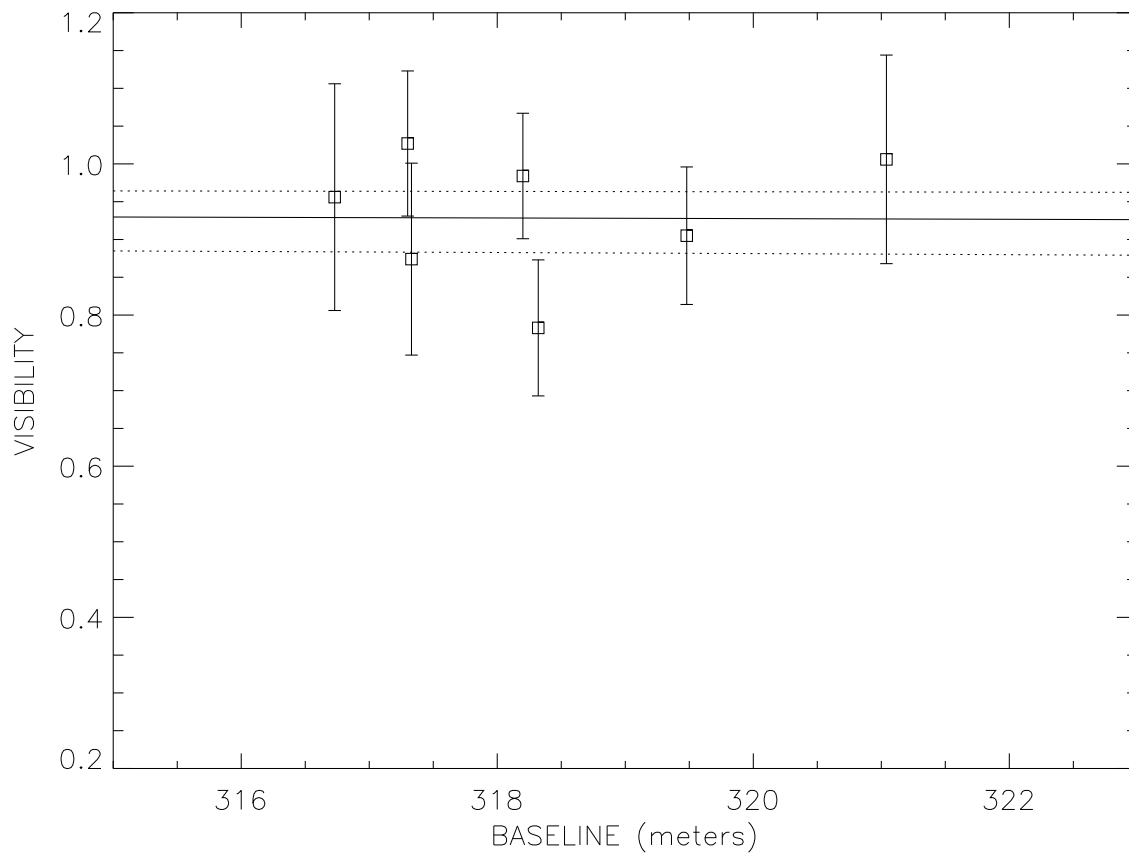


Fig. 10.— HD 50554 limb-darkened disk diameter fit.

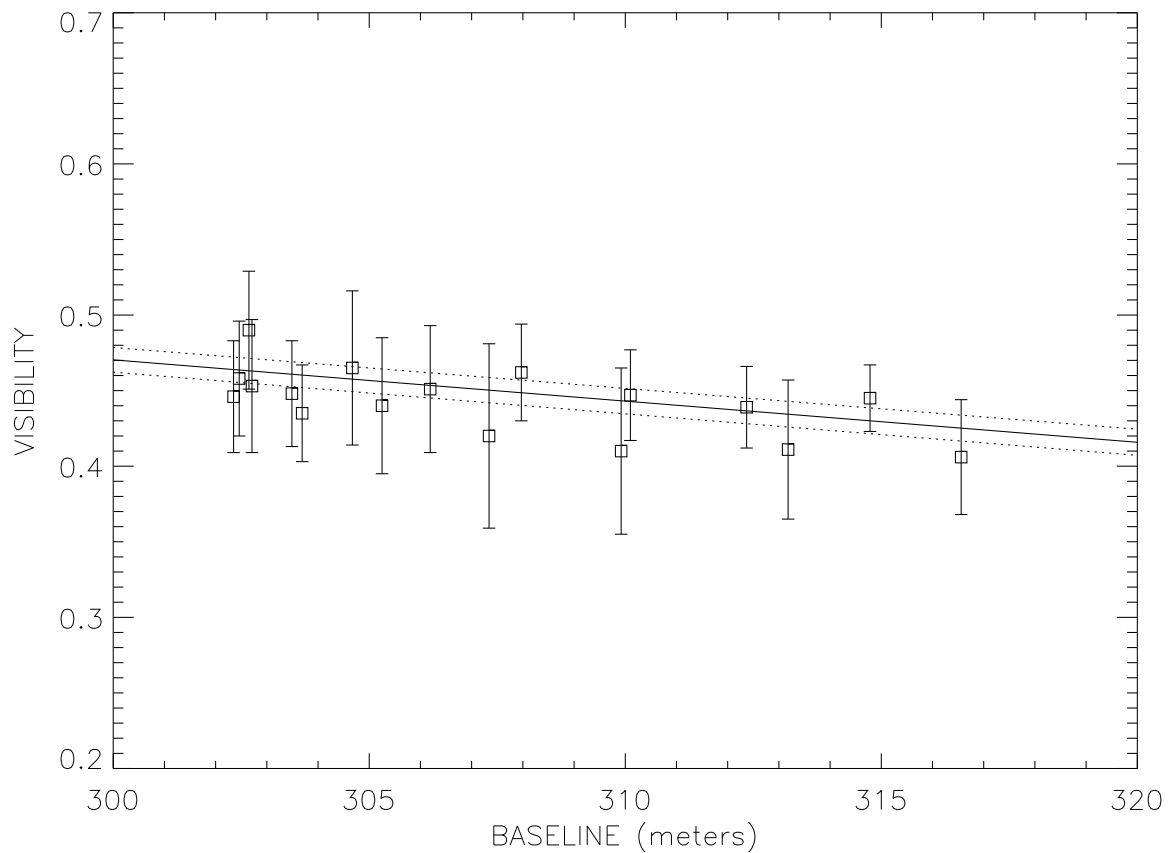
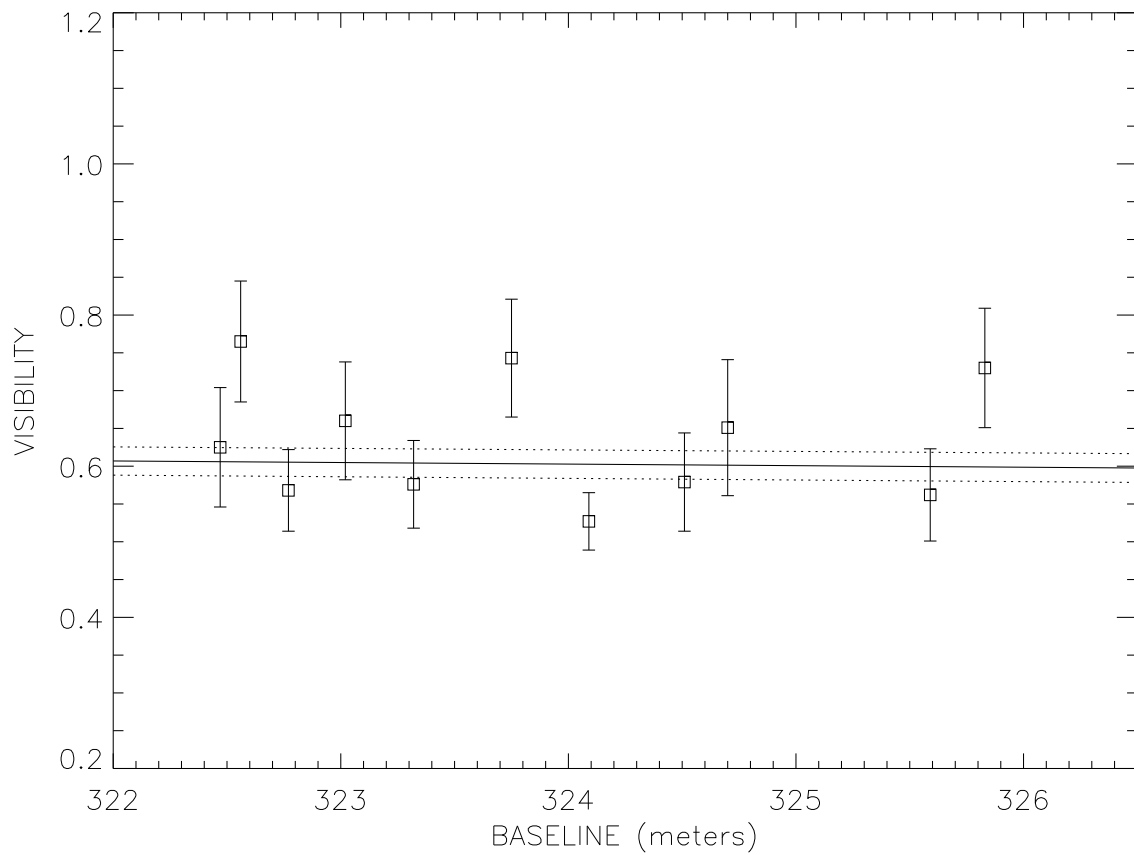


Fig. 11.— HD 59686 limb-darkened disk diameter fit.



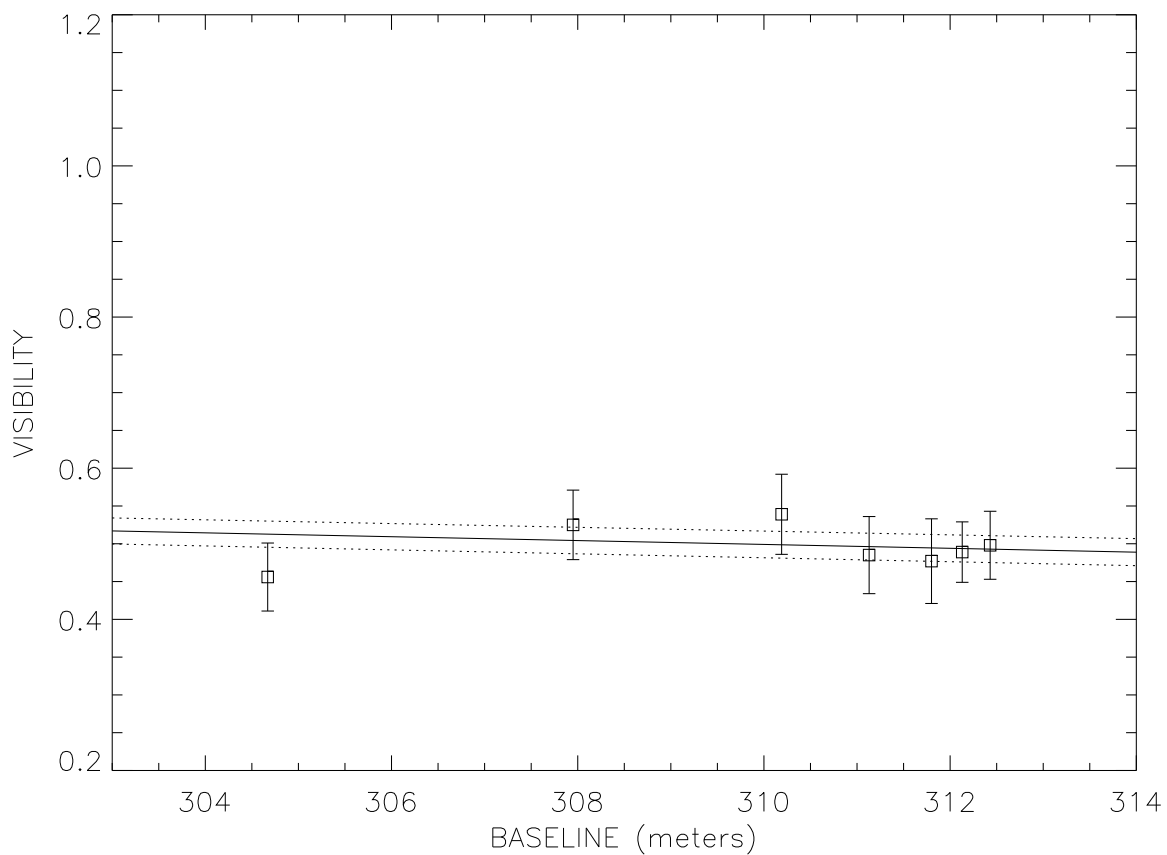


Fig. 13.— HD 104985 limb-darkened disk diameter fit.

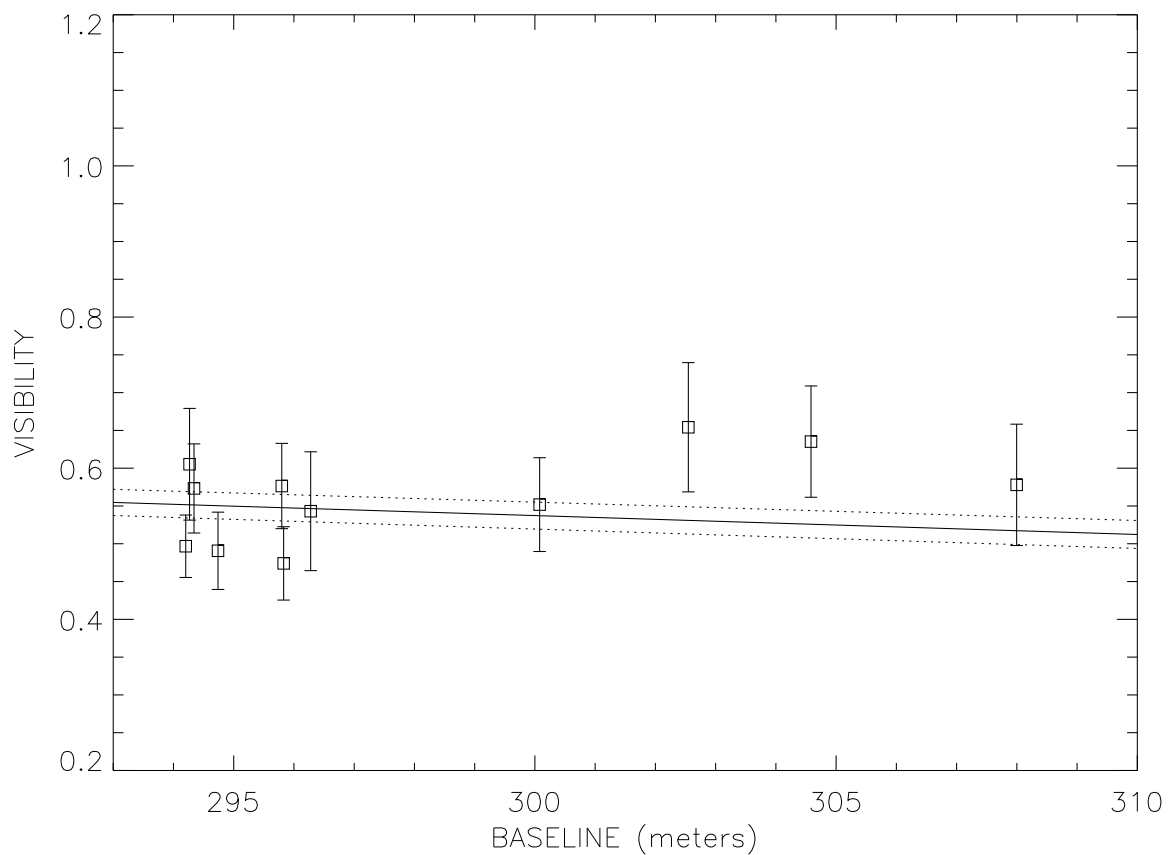


Fig. 14.— HD 117176 limb-darkened disk diameter fit.

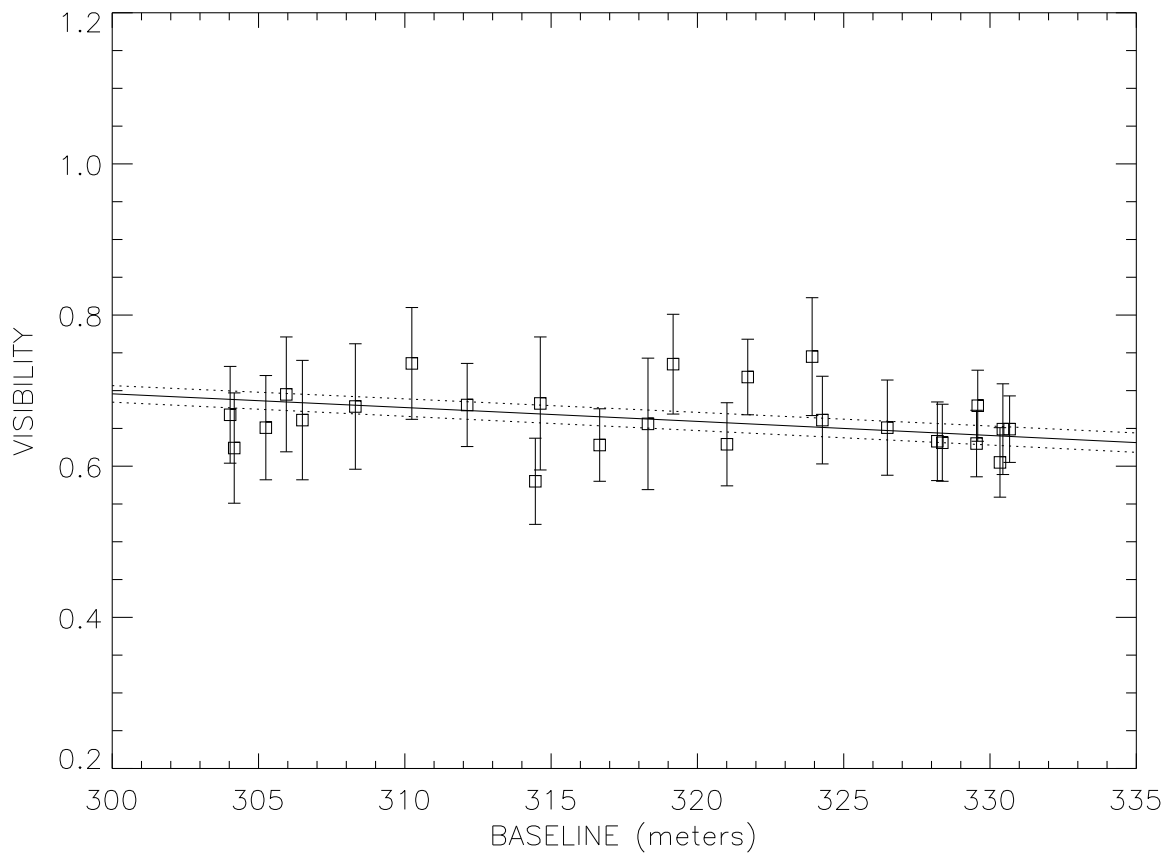


Fig. 15.— HD 120136 limb-darkened disk diameter fit.

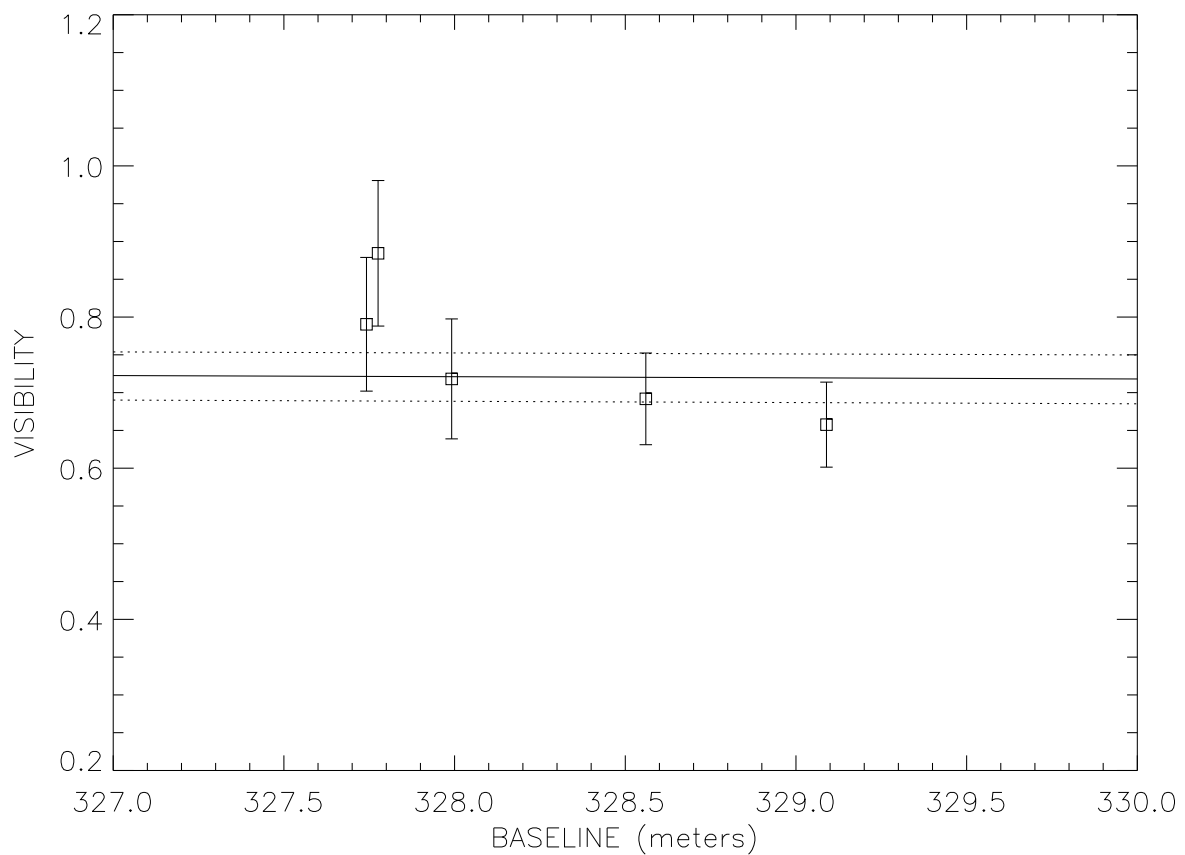


Fig. 16.— HD 143761 limb-darkened disk diameter fit.

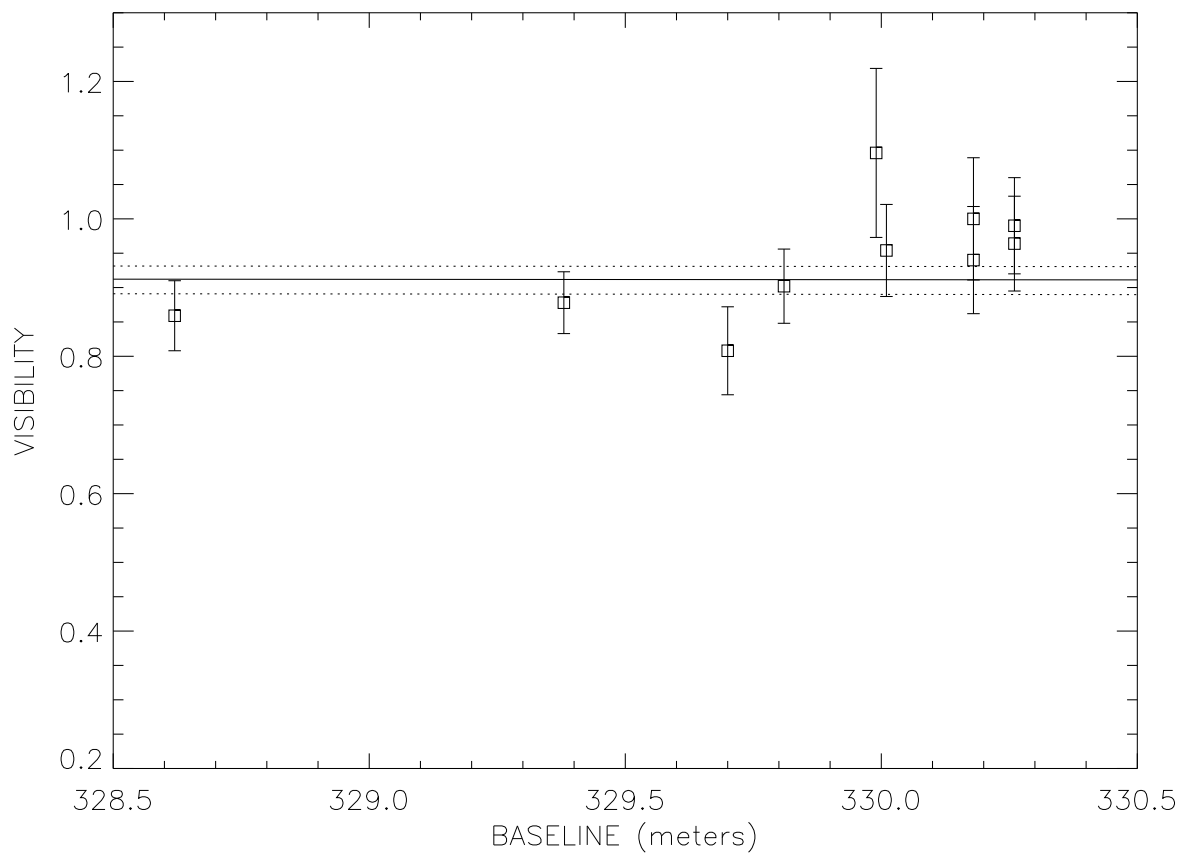


Fig. 17.— HD 145675 limb-darkened disk diameter fit.

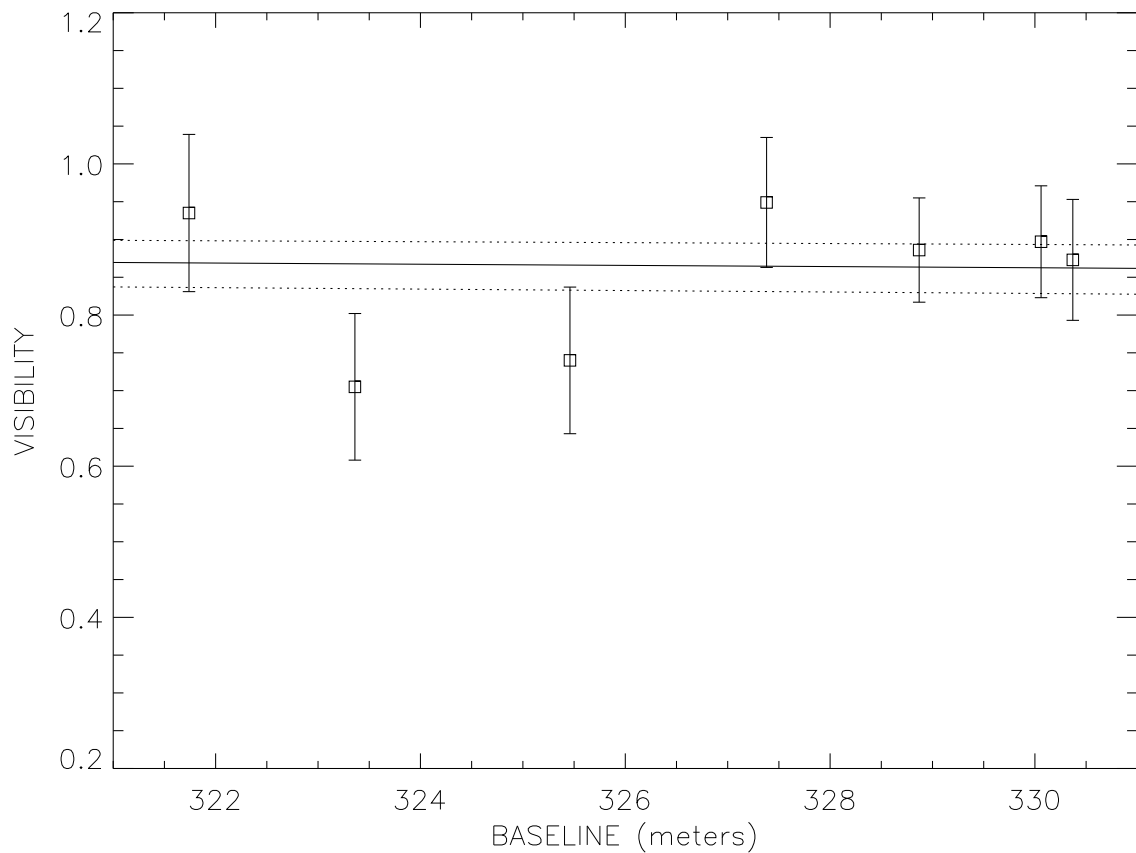


Fig. 18.— HD 177830 limb-darkened disk diameter fit.

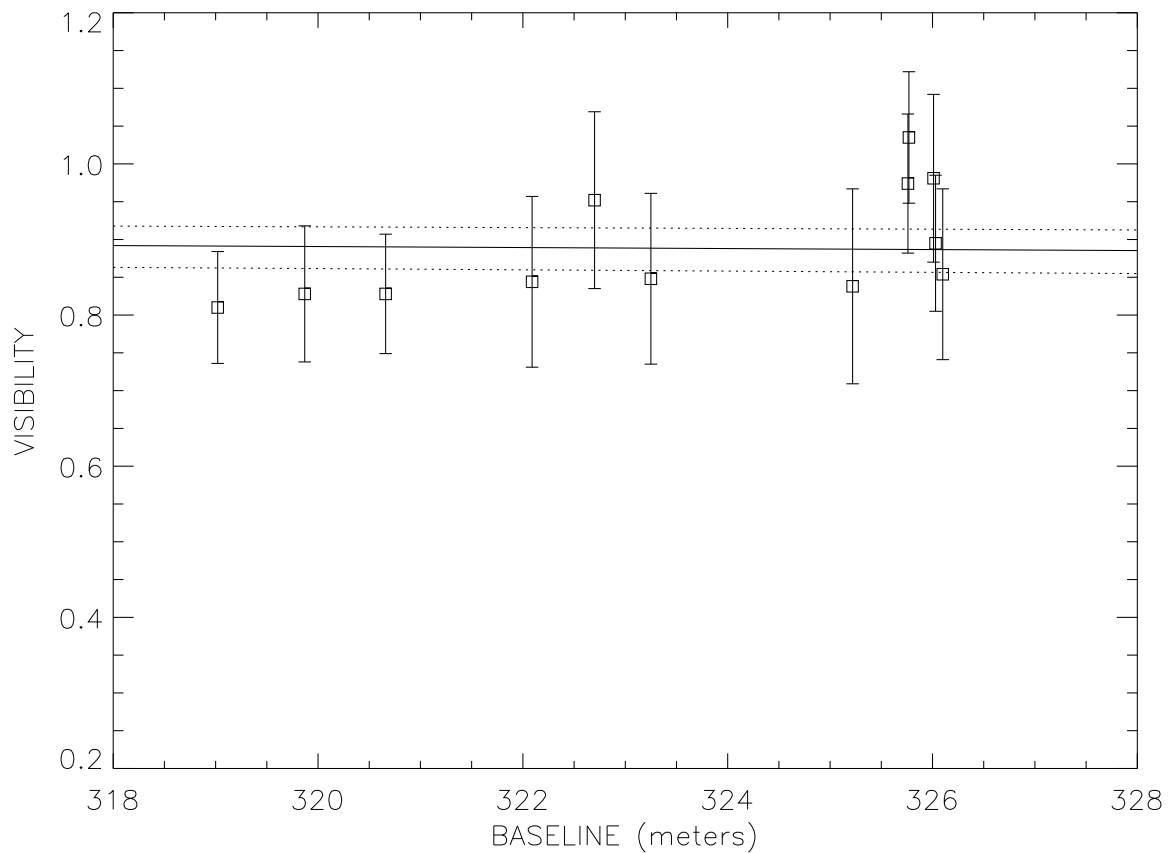


Fig. 19.— HD 186427 limb-darkened disk diameter fit.

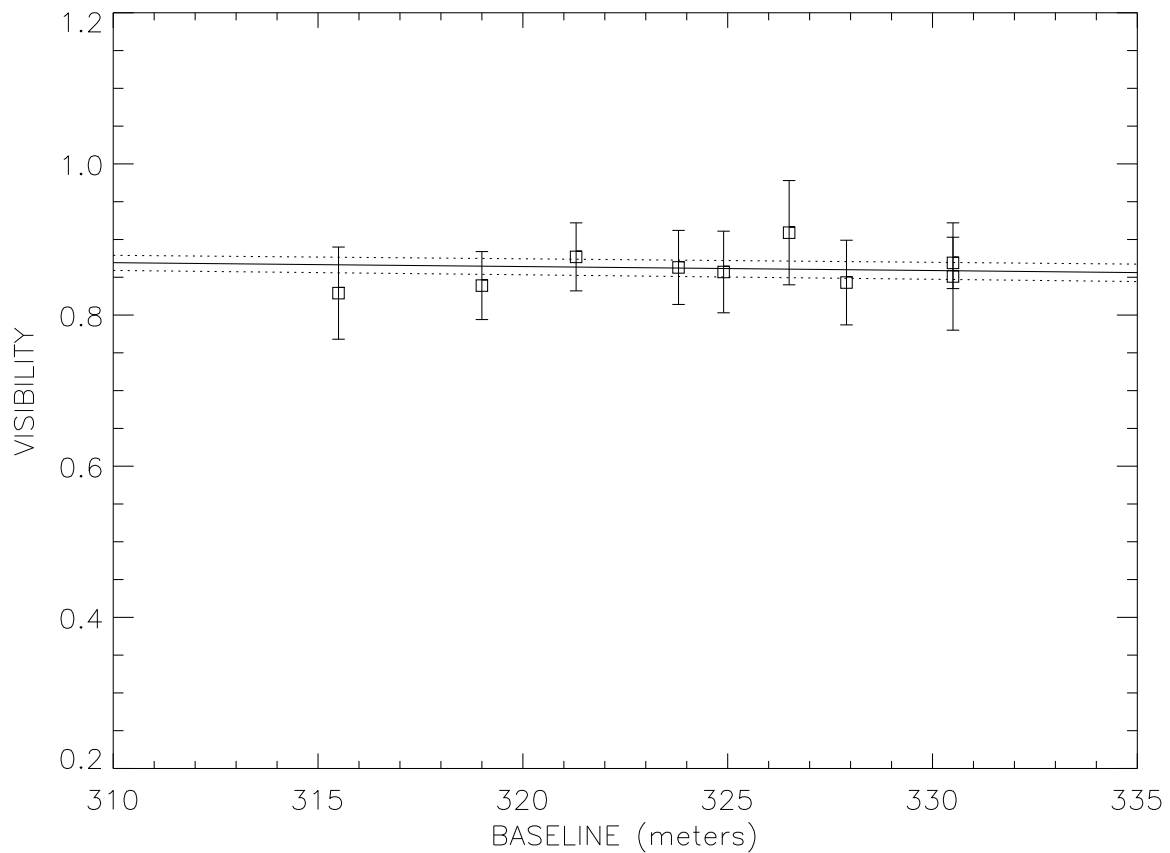


Fig. 20.— HD 189733 limb-darkened disk diameter fit.

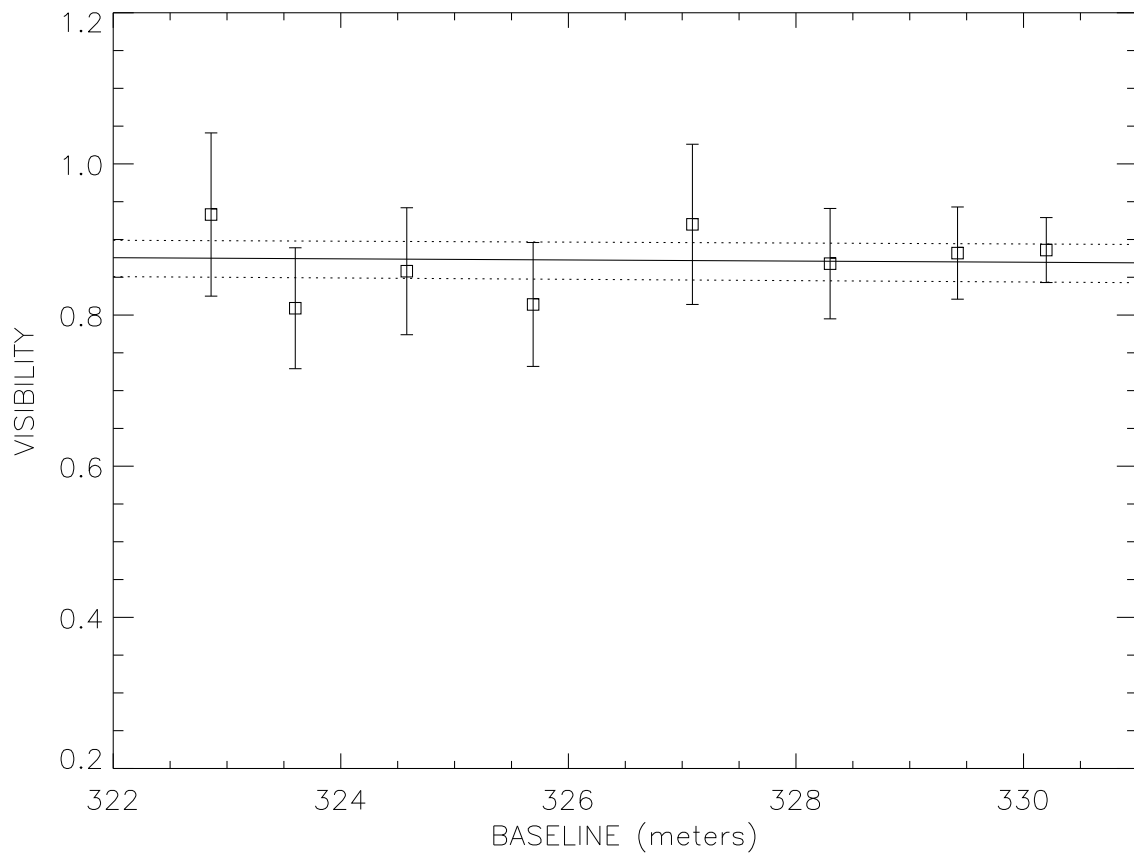


Fig. 21.— HD 190228 limb-darkened disk diameter fit.

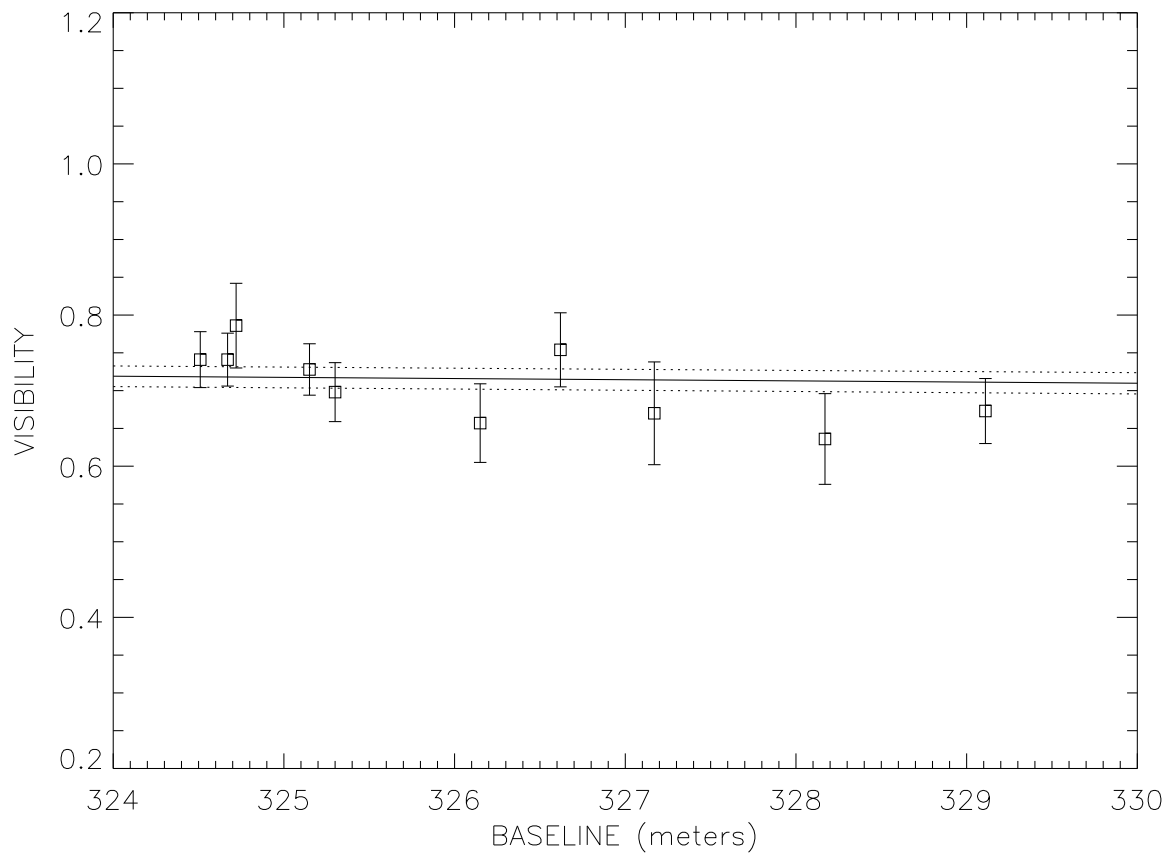


Fig. 22.— HD 190360 limb-darkened disk diameter fit.

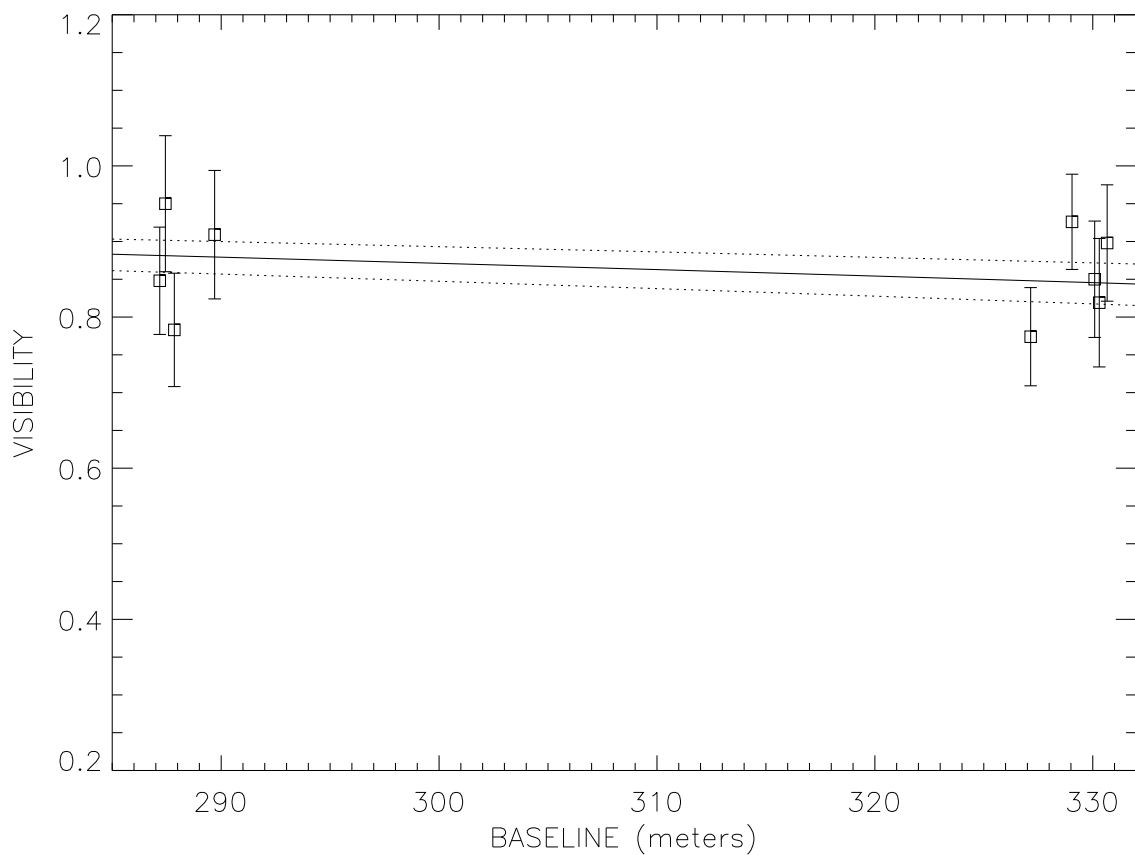


Fig. 23.— HD 196885 limb-darkened disk diameter fit.

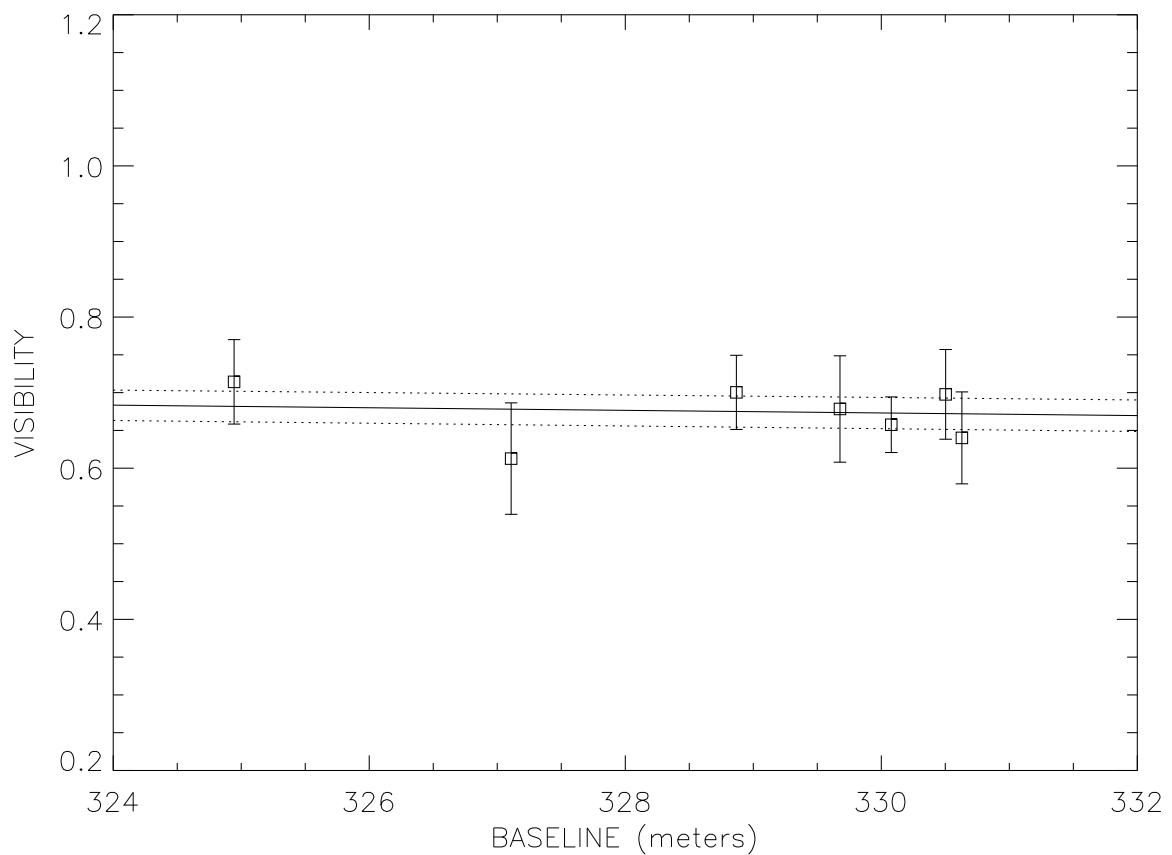


Fig. 24.— HD 217014 limb-darkened disk diameter fit.

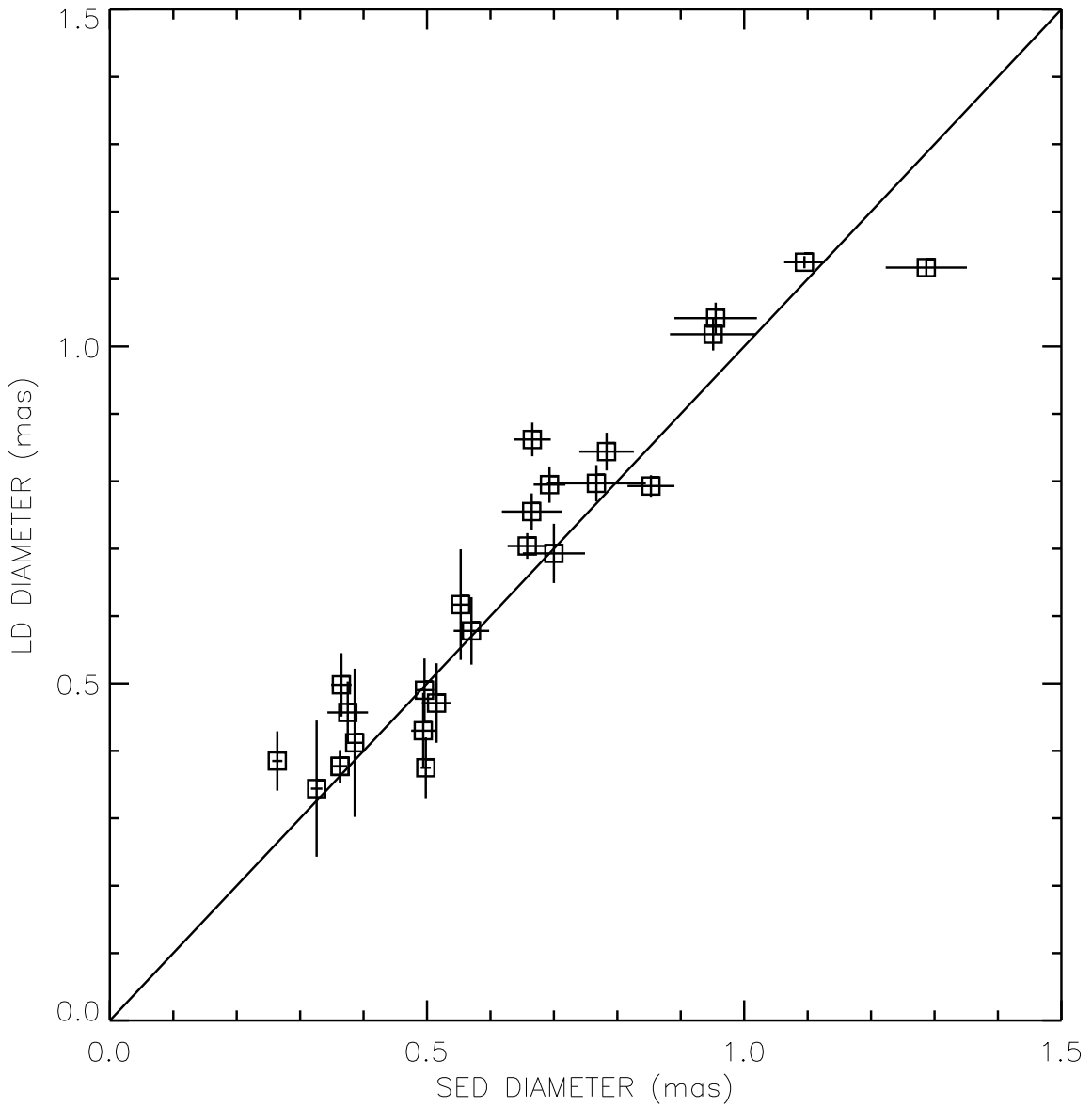


Fig. 25.— A comparison of estimated SED diameters and measured LD diameters. The solid line indicates a 1:1 ratio for the diameters. Note that at  $\theta > 0.6$  mas, the errors for the measured LD diameters become equal to or smaller than the errors from the SED diameter estimates.

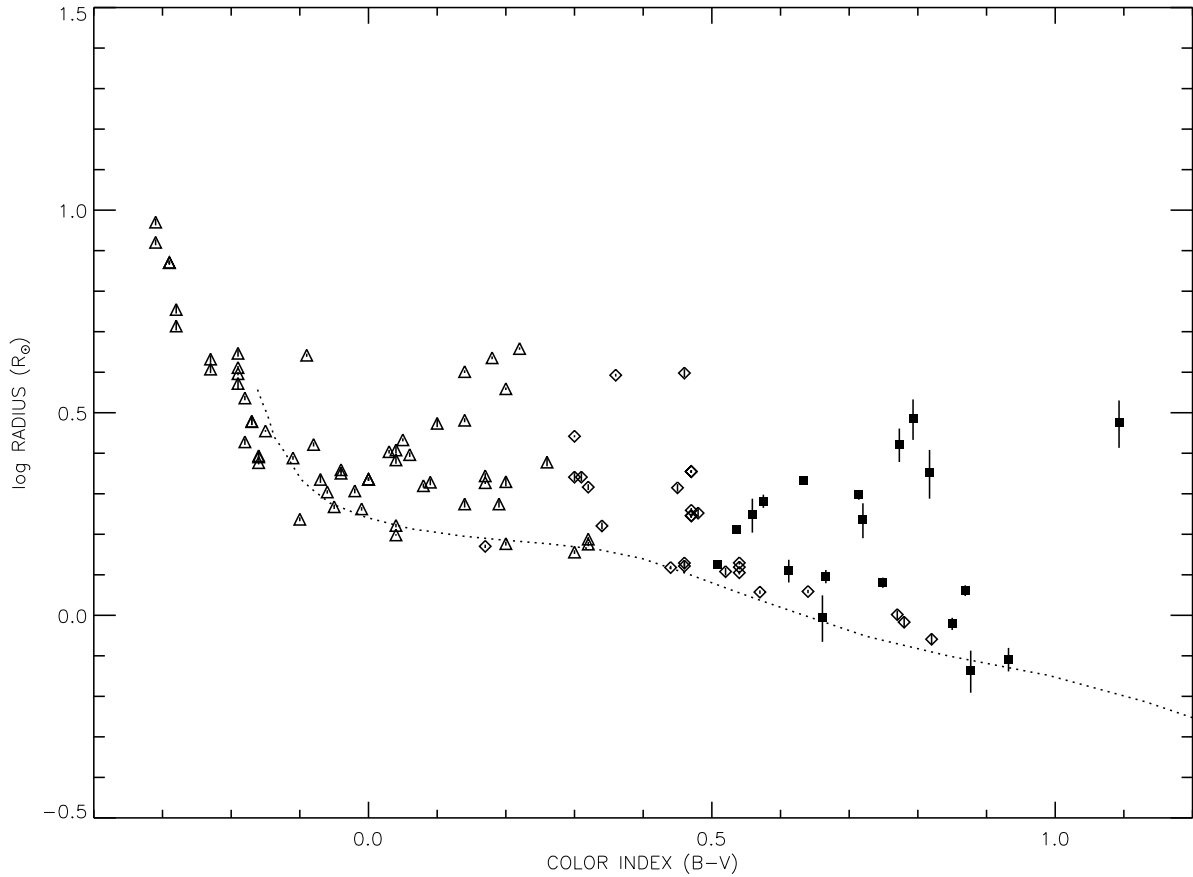


Fig. 26.— Stellar radii:  $\log R$  vs. unreddened color index ( $B - V$ ). The  $\Delta$ s represent O, B, and A-dwarf stars from the Andersen sample (Andersen 1991);  $\diamond$ s represent F, G, and K-dwarf stars from the Andersen sample; and the filled  $\square$ s represent exoplanet host stars' diameters measured here with errors  $<15\%$ . The dotted line indicates the ZAMS for stars with masses between  $0.15$  and  $5.0 M_{\odot}$  (Girardi et al. 2000).

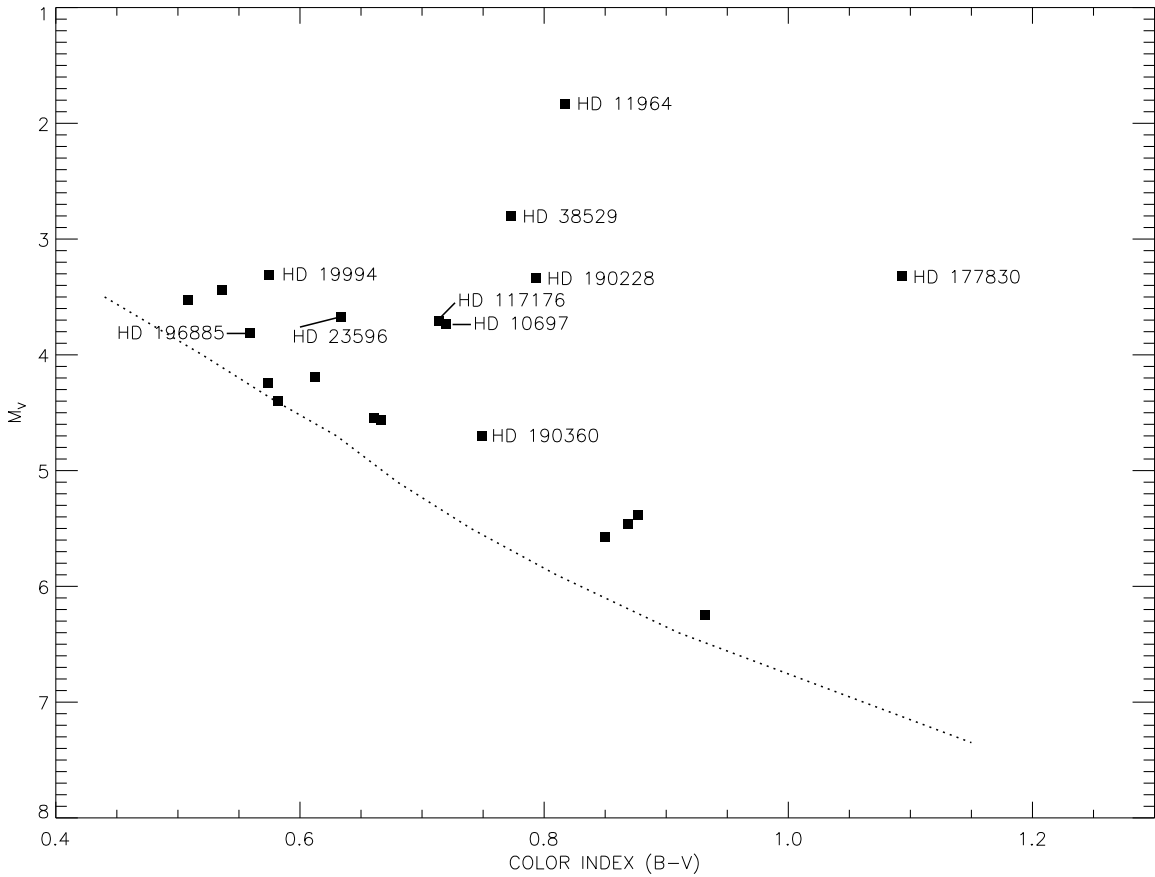


Fig. 27.— Absolute  $V$  magnitude vs. color index ( $B - V$ ). The dotted line indicates the ZAMS derived from Cox (2000). The unlabeled points are dwarfs with no problems in their measured radii. HD 10697, HD 11964, HD 38529, HD 177830, and HD 190228 are confirmed subgiants, while HD 19994 and HD 117176 are stars showing signs of post-M-S evolution. See §4.1 for details on these stars and on HD 23596, HD 190360, and HD 196885.